21GRD03 PaRaMetriC

D1: Report on the collection and production of candidate PRC materials, and identification of figures of merit to evaluate their cooling performance

Lead participant for the deliverable: **INRIM**

Due date of the deliverable: 31/10/2023

Actual submission date of the deliverable: 04/11/2023

Confidentiality Status: PU - Public, fully open

Glossary

ASTM	American Society for Testing and Materials
CDD	Cooling degree day
CR	Contrast Ratio
DLR	Downwelling longwave radiation
ECMWF	European Centre for Medium-Range Weather Forecasts
ERA5	ECMWF Reanalysis v5
IRT	Infrared transmittance
LWIR	Long-wave infrared
MTD	Maximum temperature drop
MODTRAN	Moderate Resolution Transmission
NRHEC	Non-radiative heat exchange coefficient
PDRC	Passive daytime radiative cooling
PE	Polyethylene
PFAS	Perfluorinated alkylated substances
PMMA	Polymethylmethacrylate
PVDF	Polyvinylidene fluoride
RC	Radiative Cooling (figure of merit)
RRTM	Rapid Radiative Transfer Model
RTTV	Roof thermal transfer value
SRI	Solar reflectance index
TWC	Total water content
TCWV	Total column water content
UV	Ultra-violet
VT	Visible transmittance

TABLE OF CONTENTS

1   Summary

Passive radiative cooling materials represent an emerging technology that can provide sub-ambient cooling by dissipating heat as radiation through the long-wave infrared transparency window of the atmosphere. As such, they hold promise to alleviate our growing cooling needs and could find application in a broad range of areas including, prominently, the building sector. However, due to the strong variability of this effect several external conditions, clear figures of merit and standardised testing methods to evaluate their real-world cooling performance are still lacking. In this report, we review this rapidly expanding field from the specific viewpoint of the European Partnership on Metrology project PaRaMetriC, which aims at developing a metrological framework to classify and compare these materials. Aspects related to the relevant classification criteria, boundary conditions, possible reference materials, figures of merit and methods for their determination are discussed, highlighting some of the main open questions in the field and recommended practices for their characterisation.

2 Introduction

Passive radiative cooling (PRC) is a technology that leverages the radiative cooling capacity of materials to dissipate their heat radiatively towards a cold heatsink, allowing them to potentially reach an equilibrium temperature below that of the surrounding environment, without relying on external energy sources. This phenomenon relies on the ability of specific materials to emit infrared radiation selectively in the wavelength range between 8 – 13 µm, also known as the longwave infrared (LWIR) atmospheric window. In this wavelength range, which overlaps with the blackbody spectrum of objects at ambient temperature, the gas species of our atmosphere do not have prominent absorption bands, allowing any thermal emitted radiation to reach outer space which acts as an infinite heat sink. The key to PRC technology is therefore represented by a high and possibly selective emissivity in the 8 – 13 µm wavelength range, and an unobstructed access to a clear sky to efficiently radiate heat to outer space.

While sub-ambient passive radiative cooling is well documented since ancient times during the night, the prospects of achieving the same effect during daytime hours (or even under direct sunlight illumination) were the subject of intense research efforts in the past decade, driven by the development of advanced micro and nanofabrication techniques. In order to achieve passive daytime radiative cooling (PDRC) below ambient temperature under direct solar radiation, a material should exhibit vanishing absorptivity across the whole solar spectrum (0.3 – 2.5 µm), as well as a high emissivity in the LWIR transparency range (8 – 13 µm). In recent years, several strategies have been devised to achieve these properties in a wide range of materials and architectures, ranging from multilayer stacks, to porous polymeric coatings, paint-like systems, and micropatterned metasurfaces, to name a few. Classification schemes of the materials in terms of their architectures and specific applications are therefore needed.

In addition to the material aspects, experimental research on PDRC technology requires careful consideration and a comprehensive definition of the relevant boundary conditions that can affect cooling performance. These may include the temperature measured both inside and outside the cooled space/substrate, the different degrees of insulation from other radiation, conduction and convection channels, but also the monitoring of solar irradiation, wind, humidity, cloud cover and the relative orientation between the sky and the radiative emitter. Controlling and harmonising these boundary conditions is critical to ensuring accurate, reliable, and meaningful experimental results.

The performance of novel PDRC materials can be evaluated or inferred using a multitude of different techniques involving both indoor characterization and outdoor experimental conditions. This variability in the testing conditions makes it difficult to compare different materials and predict their effectiveness under diverse conditions. The identification of meaningful and robust figures of merit for PDRC materials is a crucial task in their successful application, further development, and commercialization. Some of the main figures of merit that are currently used in the literature include spectral properties of the materials, observed temperature drops when exposed to the sky or to other heat sinks, or equivalent cooling power dissipated at ambient temperature, as well as many others depending on the targeted application.

Overall, PDRC technology has the potential to reduce cooling energy demands and mitigate the urban heat island effect, significantly reducing cooling-related emissions of greenhouse gases while improving human comfort and air quality in urban environments. This report aims to identify the classification schemes, boundary conditions and figures of merit of PDRC materials that can help define and expand the potential of this promising technology. At the same time, this document will also provide a shared knowledge base for the 21GRD03 PaRaMetriC project, and determine its area of focus.

3 Theoretical background

Kirchhoff's law of thermal radiation states that any material at thermodynamic equilibrium with a temperature higher than 0 K constantly absorbs and emits electromagnetic radiation. This emitted radiation allows bodies at different temperatures to exchange heat even in the absence of conduction and convection channels. The average temperature of the Earth, around 300 K, is mainly the result of its radiative balance with the radiative heat gains from the Sun (~5700 K) and the radiative losses towards outer space (~3 K), acting as an infinite heat sink. During the night, or even during the day if solar light is completely reflected, a material that is properly insulated from non-radiative heat gains will be able to dissipate radiatively more energy than it receives from the environment, thus decreasing its temperature spontaneously without any energy input [1].

3.1 Solar reflectance and thermal LWIR emittance

In order to achieve a net PDRC effect, the optical performance of the coating must be precisely engineered across a broad spectral range. The most-commonly defined ideal spectrum for a PDRC coating is characterised by the complete reflection of all solar irradiance (most of which falls between 0.3 – 2.5 µm) and by a perfect emissivity/absorptivity in the LWIR atmospheric window (8 – 13 µm), as shown schematically in Figure 1a. The emittance in other mid-infrared wavelengths (2.5 – 8 µm and above 13 µm), should be low enough to prevent overheating from the downwelling atmospheric irradiance and or from any residual solar irradiance. The solar reflectance ($\bar{R}_{\text{solar}}$) and thermal LWIR emittance ($\bar{\varepsilon}_{\text{LWIR}}$) are therefore the main parameters taken into account for the design of efficient PDRC materials. $\bar{R}_{\text{solar}}$ is typically defined as the ratio of reflected solar intensity to integral solar intensity in the range (0.3 to 2.5 µm), i.e. as

$$\bar{R}_{\text{solar}} = \frac{\int_{0.3\,\mu\text{m}}^{2.5\,\mu\text{m}} I_{\text{solar}}(\lambda)\,R(\lambda)\,\mathrm{d}\lambda}{\int_{0.3\,\mu\text{m}}^{2.5\,\mu\text{m}} I_{\text{solar}}(\lambda)\,\mathrm{d}\lambda}, \qquad (1)$$

where $I_{\text{solar}}(\lambda)$ is the ASTM G173-03 global solar intensity spectrum at AM 1.5 and $R(\lambda)$ is the spectral reflectance of the coating. Similarly, $\bar{\varepsilon}_{\text{LWIR}}$ is defined as

$$\bar{\varepsilon}_{\text{LWIR}} = \frac{\int_{8\,\mu\text{m}}^{13\,\mu\text{m}} I_{\text{bb}}(T,\lambda)\,\varepsilon(T,\lambda)\,\mathrm{d}\lambda}{\int_{8\,\mu\text{m}}^{13\,\mu\text{m}} I_{\text{bb}}(T,\lambda)\,\mathrm{d}\lambda}, \qquad (2)$$

where $I_{\text{bb}}(T,\lambda)$ is the spectral intensity emitted by a standard blackbody with temperature T and spectral emittance of the sample $\varepsilon(T,\lambda)$.

To achieve a measurable PDRC performance under direct sunlight illumination, $\bar{R}_{\text{solar}}$ should be typically higher than ~0.95 whereas($\bar{\varepsilon}_{\text{LWIR}}$ should reach above 0.7 (preferably > 0.9) [2].

3.2 Power balance

The net cooling power P_{net} exerted by an emitter can be calculated as a power balance between the heat losses and heat gains from the environment (Figure 1b):

$$P_{\text{net}} = P_{\text{rad}} - P_{\text{atm}} - P_{\text{sun}} - P_{\text{nonrad}} \qquad (3)$$

where P_{rad} is the thermal radiation power from the emitter, P_{atm} and P_{sun} are the absorbed powers from the atmospheric and solar irradiations, and P_{nonrad} denotes the non-radiative heat transfer processes (convection and conduction) between the coating and ambient environment.
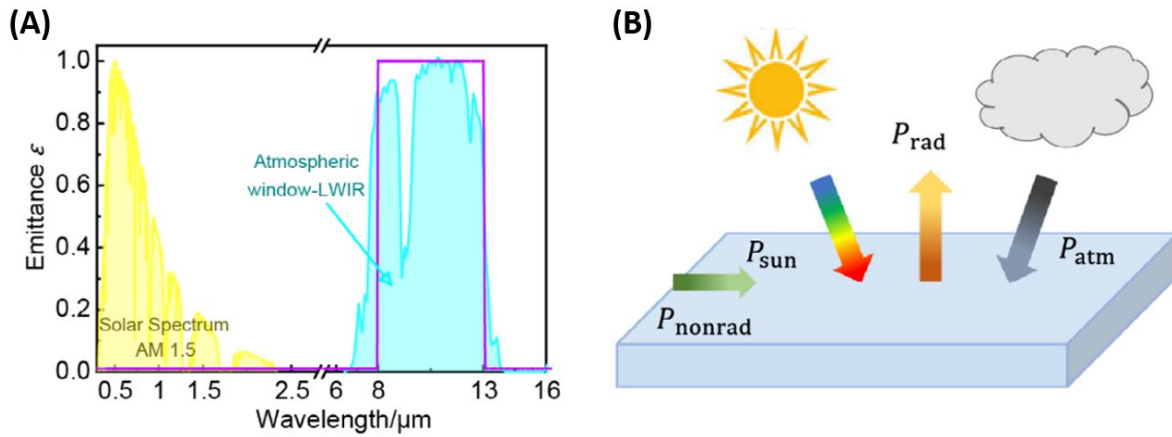
Figure 1: Fundamentals of PDRC. (A) Normalised solar spectral intensity and LWIR atmospheric transparent window represented by the yellow and green curves, respectively. An ideal emissivity spectrum of the PDRC coating is represented within the purple box. (B) Schematic diagram and heat transfer processes of PDRC coatings [1].

For an ideally working PDRC system, P_{rad} is absorbed by the atmosphere and the universe, which can be considered a "blackbody system" with unit emissivity. A fourth-power relationship exists between the radiation power and temperature, hence higher radiation power can be achieved at a higher temperature of the material. P_{atm} and P_{sun} both lower the net cooling power and can be affected by various geoclimatic conditions, such as atmospheric transmittance, solar irradiance, total precipitable water, cloud cover, latitude and zenith angle. Non-radiative heat transfer between the material and the surroundings is expressed by P_{nonrad} and depends on the temperature difference ($T_{amb} - T_{material}$) as well as on the non-radiative heat transfer coefficient h_c which is sometimes used to subsume both conduction and convection contributions. At sub-ambient stagnation temperatures, both these terms will contribute to heating the material, and should be therefore minimised by properly insulating the overall cooling system.

4   Classification schemes and selection criteria

In a time span of just a few years, PRC materials have grown into a broad family of very heterogeneous materials, in terms of the number of their components, their composition, mechanical and spectral properties, and targeted application. Accordingly, several criteria can be devised to classify them into different groups. In the following section, we will identify the most relevant criteria for the specific scope of our project, which focuses on energy efficiency and energy saving of cooling appliances in the building sector. Given this context, our classification criteria (and proposed figures of merit) may not fit equally well all the additional application areas of PRC materials that have been demonstrated in recent years. Notable examples include, for instance, the quickly growing field of PRC textiles and personal thermal management, or the development of PRC materials targeting specific applications such as water harvesting, thermoelectric generation, or the cooling of photovoltaic cells (which requires PRC materials that are transparent at solar wavelengths). In consideration of the above, we identify the following main criteria for the classification of PRC materials and their testing within the PaRaMetriC project.

4.1   Period of use

The cooling potential of PRC materials is highest during the night, and as such was already documented for night-time ice-making purposes in ancient Persia and India [3]. The first systematic approach to the night-time cooling of material surface below ambient temperature dates back to the 1970s. During the same years, the first demonstrations of daytime sub-ambient cooling were also prospected, albeit only for materials shielded from direct sunlight illumination [4]. Extending the application to daytime use was a significant challenge due to the negative effect of solar irradiation on the cooling performance. In order to achieve sub-ambient radiative cooling under direct sunlight illumination, materials need to possess vanishing solar absorptivity, a condition which is extremely challenging to fulfil consistently across such a broad wavelength range. This result was finally demonstrated for the first time in 2014 in a seminal work by Stanford University [5] based on a multilayer stack deposited on a silver mirror which was able to reflect 97 % of incident sunlight, reaching a stagnation temperature 4.9 °C below ambient under a peak irradiance of 900 W m^{-2}. Since this first demonstration, the field of PDRC materials has attracted an increasing interest of the scientific community, due to its promising prospects of significantly reducing our energy-intensive cooling needs. Due to their relevance, the scope of the PaRaMetriC project focuses primarily on materials that are capable of daytime cooling, possibly under intense (> 900 W m^{-2}) direct illumination conditions.

4.2   Applications

One of the main applications of PDRC materials is in the building sector, to reduce the cooling needs or improve the energy performance of existing cooling appliances. An early estimate commissioned from the U.S. Department of Energy estimated projected electricity savings between 45 and 68% across different US cities for the case of a medium-sized office building when adding a hydronic radiant system using PDRC materials to a traditional variable-air-volume system [6], with more recent works suggesting savings up to 80 % with optimised or concentrated geometries [7]. During the day, roofs of most residential, commercial and industrial structures can heat to very high temperatures due to solar radiation. The resulting heat is then released in the environment (contributing to the heat island effect), or can be transferred to the internal living space, exacerbating cooling demand. Traditional "cool roof" paints have existed in the market for a long time. Analogously to the case of PDRC materials, these paint products are also characterised by high LWIR emissivity and solar reflectivity, typically above 80 %. The combination of these two properties is typically summarized by their solar reflectance index (SRI), a parameter which expresses the ability of the material to maintain a low surface temperature under certain standardised solar irradiance and convection conditions, as defined in the ASTM E1980-11 standard. High-performing "cool roof" paints are typically characterised by SRI values around or slightly above 100, which however are not sufficient to achieve sub-ambient PDRC. The ubiquitous presence of TiO_2 nanoparticles in most paint formulations is now commonly believed to be one of the reasons limiting the thermal performance of these products, due to their absorption in the UV range [8]. Therefore, while certainly beneficial to reduce cooling needs, traditional "cool roof" paints can only limit overheating rather than offer a net cooling. Covering roof areas directly with PDRC coatings holds promise to further increase the albedo of our urban environments and limit electricity consumption during heat waves.

Figure 2: PDRC for building cooling – energy balance for a radiative roof surface [1].

Albeit apparently straightforward, the direct application of PDRC coatings on buildings may not be the most effective strategy to reduce cooling needs in several contexts. Modern buildings have at least some degree of thermal insulation in their walls and roofs which limits the possibility of actually cooling the living spaces by simply applying a highly emissive paint on their external surfaces. Even for less insulated spaces, the direct application of PDRC materials could introduce undesired cooling effects, which may offset the expected energy savings by aggravating heating needs during the night or in winter. Hence, it can be envisioned that the purely passive applications of PDRC materials will be sought in scenarios requiring the dissipation of endogenous heat, such as electric distribution boards, power conditioning units or data centres.

Next to the passive approach [9], in which the roof is covered with PDRC coating to drain heat directly from the internal space (Figure 3b) or PDRC materials are used to induce a fully passive circulation of cooled air [10-11], active systems [12] were also proposed (Figure 3a). These designs are based on liquid cooling, which was also studied extensively [13]. In this case, heat is transferred across the system by a liquid, which is cooled down by PDRC. Even though a small energy input is needed for circulating the liquid, cooling can be better controlled and easily regulated in active systems, as well as combined with cold liquid storage options (e.g., to use the cooling power accumulated at night during daytime hours). The generated cold liquid could be then used in a closed-loop (i.e., with no net water consumption) to drain heat directly from the space to be cooled [14], or to lower the temperature of the condenser unit of traditional heat pumps to increase their coefficient of performance, thus lowering their electricity consumption [15].
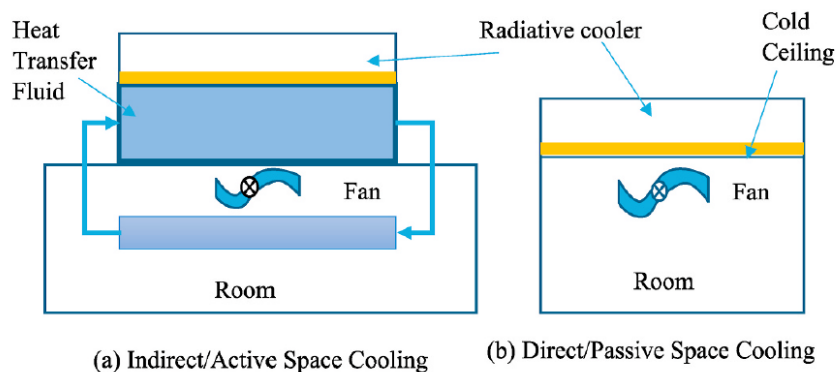

Figure 3: (a) Active PDRC system using liquid circulation, (b) passive PDRC system [16].

As discussed previously, other PDRC applications include personal thermal management with clothing and wearables [17], solar cell cooling [18], harvesting water from the atmosphere [19], protecting ice from melting [20], direct electricity generation [21] and water desalination [22].

In certain specific cases, additional and more application-specific spectral constraints could apply such as for cooling materials in the photovoltaic field (which should reject only the sub-bandgap spectral range of solar light) [23], or in the agricultural sector for mitigating water scarcity (e.g., using mulching or greenhouse films that allow only solar wavelengths useful for photosynthesis) [24], or finally for spacecraft thermal management (where broadband emissivity is always preferred due to the absence of the atmosphere) [25].

The performance evaluation methods under development in PaRaMetriC may still be relevant to some of these additional applications, which however remain outside of the main scope of the project. In particular, some of these applications are targeting radiative cooling at above-ambient conditions, or require free-standing and thermally insulating materials which may still be capable of cooling themselves or avoid overheating by shielding solar gains, but not to drain and dissipate heat efficiently from a thermal load applied to them. In general, PaRaMetriC will focus on materials which can also provide cooling at ambient conditions, and which can efficiently exert their cooling power when put in thermal contact with a thermal load. This is identified as a basic condition for the accurate measurement and future utilisation of PDRC in many practical applications.

4.3   Materials and structures

The two main parameters required for the realisation of PDRC are an exceptional reflectance at solar wavelengths, and a strong and preferably selective emissivity in the atmospheric window (8 – 13 µm). To achieve strong solar reflectance, two main strategies consist of using metal reflectors (Ag or Al), or broadband diffuser comprising polydisperse dielectric nano- and micro-particles or, conversely, nano- and micro-pores in a host matrix [1]. In this case, all materials involved are typically highly transparent polymers [26], or dielectrics exhibiting a large band-gap to avoid undesired absorption at UV and near-UV wavelengths [27]. Most of these materials are also characterised by a strong emittance in the atmospheric window, which helps achieve both properties at the same time.

Possible classification criteria based on the material aspects can be therefore expressed in terms of their optical mechanism for solar reflection (either specular or diffuse, even though intermediate cases are also common), or on their composition (either purely organic, inorganic, or both). These materials can be arranged in a layered/film structure (for instance, a polymer layer, a pigmented paint coating, or an inorganic multilayer stack), be made of a combination of discrete microparticles or micropatterned arrays on a surface, or spun as a fibrous material [28]. Film-based radiators exhibit generally easier production requirements and are favourable in the field of building cooling systems due to their simple application. Other advantages such as the absence of a metal reflector and better thermal contact with the substrate hold promise for their broad use, even though challenges remain in many cases for their standardisation (see Section 6). More complex materials exhibit often better spectral properties and cooling performances, but remain less accessible and harder to produce on a large scale [29].

A common example of structure-based classification of PDRC materials is found, for instance, in the review paper by Yu *et al.* [30], where four main groups are identified: multilayer structure, metamaterial, randomly distributed particle structure and porous structure. Figure 4 shows schematic representations for all the four groups.
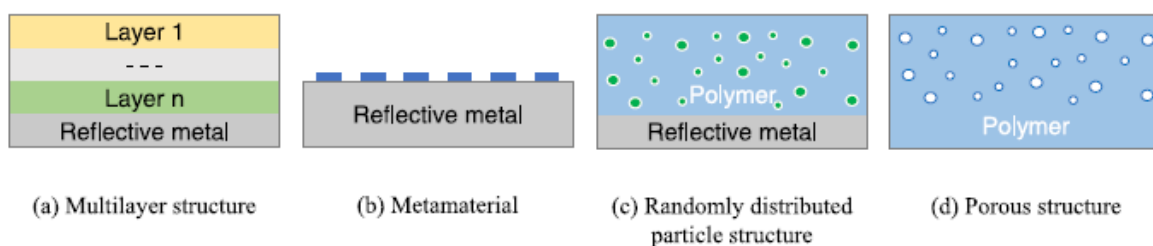

(a) Multilayer structure   (b) Metamaterial   (c) Randomly distributed particle structure   (d) Porous structure

Figure 4: Four structures for achieving PDRC [30].

For multilayer structures (Figure 4a), the bottom layer is typically made of silver to provide a high solar reflectance, while the above layers are designed to enhance emissivity in the atmospheric window via either interference effects for nm and few µm-scale layers, or bulk emissivity in the case of larger layers. The

thickness and number of layers needs to be designed to meet specific spectral properties. The possibility of utilising metamaterials (Figure 4b) has been made possible with advancements in micro and nanofabrication technology. Fabrication of precisely patterned surfaces is crucial for reaching the desired spectral response. When combined with a metal reflecting layer, these patterns are typically meant to enhance thermal emissivity/absorptivity, which typically require the patterning of individual features with sizes comparable with the infrared wavelengths. Patterned surfaces are typically associated with higher fabrication complexity and costs, even though disordered patterns have also shown to be highly effective, and self-assembly methods, roll-to-roll, sol-gel, or nanoimprint strategies show good potential for scalability [29]. Polymer-based approaches (Figures 4c and 4d) represent typically a more economical alternative which is amenable to large scale production by several methods. Thanks to the huge variety of polymeric materials, they have a great flexibility for the engineering of their emissivity, which can be made more or less selective based on the specific chemical bonds present between their constituent atoms.

Concerning polymers, one final material that is commonly associated with PDRC applications and the possible embodiments of different PDRC architectures, is polyethylene (PE). Polyethylene is the most common type of plastic and the simplest among all polymers, containing only C-C and C-H bonds. Notably, these two bonds do not present any absorption resonance within the atmospheric transparency window, which makes thin polyethylene films highly transparent in this range. For this reason, thin PE films are used ubiquitously across PDRC experiments as a physical barrier against wind, i.e., to reduce convective heat gains and make temperature measurements more stable [31]. In this respect, PE is not a PDRC material *per se*, even though it can become an integral part of the architecture of any PDRC material to enhance their cooling performance. In particular, relevant examples have been reported in the literature of porous PE films which can be either integrated on top of a highly emissive PDRC material or used as an additional cover layer, to provide additional solar reflection, thermal insulation from external air, and a hydrophobic surface finish [32-35]. Notably, large-scale production of thin nanoporous PE films is quite inexpensive, as these membranes are already used in different applications uncorrelated to PDRC.

4.4   Mode of use

One final classification criterion that is relevant to the PaRaMetriC project, is related to the intended mode of use or the architecture of the material. In general, PDRC materials that have been reported up to now can be divided in two classes, depending on whether they are available as a standalone, self-supporting material, or meant to be applied and adhere onto a substrate. Examples of the former class include for instance several textiles [36], or other remarkable materials such as delignified wood [37], as well as other types of bulk aerogels [38-39]. These materials can be characterised by exceptional solar reflectance and thermal emissivity properties, and potentially play a significant role in the building sector (either in the form of solar-reflecting awnings and tents, or as structural materials, or as insulation, etc.), however their main function is that of shedding their own heat efficiently, rather than draining it from the environment and the underlying space/substrate, due to the poor thermal contact that can be established between these materials and a thermal load.

The second broad class of PDRC materials can instead be applied on other surfaces with good thermal contact, either by casting, coating, spraying, painting, etc. During PaRaMetriC, an important criterion for the testing of the cooling performance of different PDRC materials will be related to their ability of lowering the temperature of an applied thermal load. In other words, the estimation will rely on the temperature of the thermal load, rather than the PDRC material itself. This is preferable for several practical reasons: consistent thermal contact can only be guaranteed on a standardised thermal load rather than directly on the very different types of PDRC materials. The use of a well-defined thermal load (such as a temperature-controlled water flux) can also reduce the uncertainty associated with the cooling power due to the high reliability of contact temperature measurements of liquids. Similar characterization methods may not be equally applicable to free-standing PDRC materials, which may be therefore not compatible with the testing protocols and apparatuses developed during the project.

4.5 Candidate PDRC reference materials

By its own nature, the PDRC effect requires direct access to clear sky conditions. This makes it particularly difficult to standardise the testing of these materials, since environmental conditions are not under our direct control and can vary according to several factors. Among several approaches proposed up to date towards more reproducible testing of PDRC materials (see also: Section 6.4), one of the approaches that will be pursued by PaRaMetriC is the identification of suitable candidate PDRC reference samples that can be tested alongside novel PDRC materials to make the measured data more comparable across different seasons, geoclimatic locations and weather conditions.

The most relevant properties of candidate PDRC reference materials are not necessarily the same as those of general PDRC materials. While it is of course important that these materials exhibit a very high solar reflectance and thermal emissivity, different criteria may be more relevant than their expected PDRC performance compared to state-of-the-art materials presented in the literature.

Ideally, candidate PDRC reference materials should be widely available, including either industrially produced, commercially available materials or samples that are simple to fabricate. Secondly, to accommodate the different testing apparatuses of research groups, these materials should be available or fabricable over a reasonable range of surface areas, with high uniformity. Such uniformity constraints, which include their internal composition, thickness, and surface finish, may not be always easy to achieve with some of the most easily scalable PDRC materials, such as paint mixtures. Additionally, ideal samples should exhibit a high stability with respect to their spectral, structural and thermophysical properties, to ensure that their response does not change with time or after exposure to environmental conditions. This includes, e.g., a reasonable resistance to contamination by dust, aerosols and other fine particulate matter, as well as to prolonged UV irradiation during the outdoor testing sessions. Finally, since these materials need to be applied on a substrate, the application method should also be highly reproducible and stable.

This set of criteria narrows down the selection of suitable candidate materials. Paint-like systems, for instance, have excellent scalability and low cost. However, they can be made of a large number of components, and their optical properties may depend on the details of their application method (brush, roll, spray, blade coating, etc.) and drying conditions. Moreover, in order to reach a high reflectance, very high particle volume concentrations must be used [40-41], which may compromise their stability. The number of ingredients may be reduced by realising custom paint formulations or even by synthesising directly the relevant types of nanoparticles (e.g., $BaSO_4$ or $CaCO_3$), which however may result in different granulometries across different batches.

An appealing alternative option to conventional paint formulations is represented by porous poly(vinylidene fluoride-co-hexafluoropropene) P(VdF-HFP)$_{HP}$ membranes [42], which can be conveniently obtained by a quick phase inversion process with water (nonsolvent) in acetone (solvent). The resulting material has remarkable optical properties, can be fabricated easily, and is made of just one material. PVDF co-polymers have also exceptional durability against weathering agents, are extremely stable and naturally hydro repellent. Similar to the case of many PDRC paints, at the moment, the high content of volatile solvents during the phase inversion process makes their practical application in the EU unlikely, but this may still be acceptable for the fabrication of few samples to be used as references. However, at the beginning of 2023, the European Chemical Agency has put forward a proposal for a universal ban of around 10,000 per- and polyfluoroalkyl substances (PFASs, which include most fluoropolymers used so far in the literature as PDRCs) due to the long-standing health and environmental concerns related to their use and bioaccumulation [43-44].

Silver-based reflectors complemented with an emitting layer could meet the requirement of easily obtainable and reproducible PDRC materials, with a few notable examples already proposed in the literature. Except for its intrinsic absorption at UV wavelengths, silver offers a very high and relatively constant reflectivity across all relevant wavelengths, allowing it to reflect the largest part of solar irradiance. Coating a silver reflector with a polymer layer that is highly transparent at solar wavelengths and highly emissive in the atmospheric transparency window potentially allows to obtain a simple and reproducible PDRC material. Some relevant examples include polymers with inorganic backbone such as polysiloxanes [45] or polysilazanes [46], due to their relatively selective emissivity. A particularly interesting combination (for standardisation purposes) was also proposed in the literature, using a commercial long-lasting grade of transparent scotch tape [47]. Scotch

tape is widely available, inexpensive and highly reproducible. Moreover its typical composition includes acrylic adhesive and polypropylene, which are also highly emissive components.

Interestingly, large scale films using a diffuse or silver-based reflector complemented by non-fluorinated polymer emitters are currently under development from international companies for PDRC purposes, which may become soon available and represent an excellent option for a possible candidate reference materials. Contacts have already been established with these companies, to exchange materials and proceed with their detailed characterization by the participants and collaborators of the PaRaMetriC consortium.

Finally, as an alternative to polymer-based emitters, fully inorganic layers can also be used to obtain a selective emissivity [5, 48-49]. Commonly used materials in this case are Al_2O_3, Si_3N_4, AIN or simple SiO_2 due to their pronounced bands within the atmospheric transparency window. While the controlled deposition of these materials requires dedicated equipment or production lines, the fully inorganic nature of the resulting PDRC material would be highly promising in terms of resistance to atmospheric agents and contamination, stability and uniformity. Further emissivity enhancement could be obtained by creating surface micropatterns, which however would require the use of etching techniques, even though the resulting samples may be then stored almost indefinitely for their repeated use.

Based on the above considerations, the partners in the PaRaMetriC consortium, which include companies active in the development of metalized solar reflectors and highly emissive polymers, are exploring several options for possible candidate PDRC reference materials, with a particular focus on large scale films and silvered polymer emitters.

5   Boundary conditions

With an increasing number of studies introducing various novel PDRC materials, a wider range of functionality and applications of this technology are reached. This raises the question of identifying the fundamental limitations and constraints that PDRC materials are subject to under different climates. The effect of various atmospheric and material conditions on PDRC performance is also actively studied in the literature. In the next sections, boundary conditions and limitations of sub-ambient PRDC performance regarding mostly space and liquid cooling will be presented.

5.1   Solar and downwelling longwave radiation

Even though PDRC materials are designed to have low absorptivity in the solar spectrum (0.3 - 2.5 µm), the intensity of solar irradiation has a strong impact on the cooling performance. The visual appearance of materials reflecting 96 % or 98 % of solar irradiance would be largely indistinguishable by eye, but their cooling performance would be significantly different due to the doubled solar heat gains suffered by the former. Indeed, the results of many studies show that the cooling performance of PDRC materials at sub-ambient temperatures decreases rapidly and eventually vanishes with increased solar radiation. For example, Zhao *et al.* [2] performed experiments with a silvered SiO_2 PDRC mirror under different clear sky conditions in China over a 1-year period and further investigated the phenomenon by numerical thermal simulation. Figure 5 shows the results of the equilibrium temperature (lowest temperature the emitter can reach with $P_{net} = 0$) dependence on solar radiation.
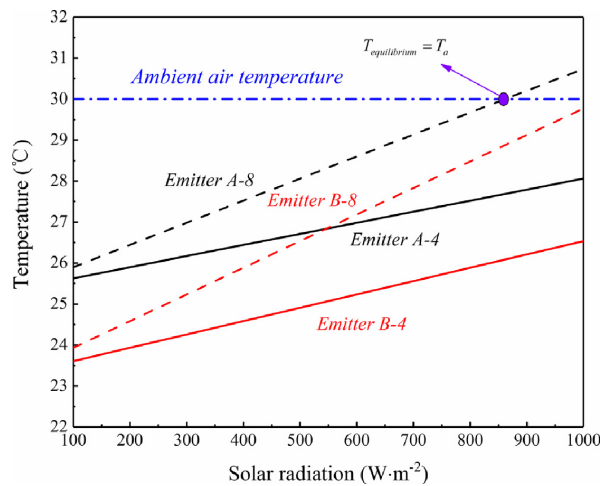

Figure 5: Equilibrium temperature of different emitters under different solar radiation [2]. Spectral properties for emitters A-4 and A-8 are retrieved from a real SiO_2 mirror measured data (average emissivity within 8-13 µm: 0.79, average solar absorption: 0.04 and 0.08, respectively), whereas emitters B-4 and B-8 represent the corresponding ideal perfect-selective materials (average emissivity within 8-13 µm: 1). During the simulation, ambient temperature was set as 303.15 K, the value of heat transfer coefficient h was set as 10 W m^{-2} K^{-1} and the precipitable water vapour was fixed at 2.0 cm.

From the numerical calculation, almost linear dependence of solar radiation on the PDRC performance is observed. For emitters with lower solar absorption (A-4 and B-4), cooling is achieved and maintained even under 1000 W m^{-2} solar radiation. However, for emitters with higher absorption (A-8 and B-8), the cooling capacity is quickly lost with increasing solar irradiance, eventually reaching an equilibrium temperature that is higher than ambient air temperature. These results emphasise near-perfect solar reflectivity as a crucial parameter for PDRC applications in regions with strong solar irradiation.

Thermal irradiance received from the atmosphere is another main factor determining the final cooling performance of a PDRC material. In a work from Feng *et al.* [50], a thermal model was used to simulate cooling performance of three PDRC materials in three different climates, mild (Sydney, Australia), desertic (Alice Springs, Australia) and tropical (Singapore). To evaluate the influence of downwelling longwave radiation (DLR), a sensitivity study was performed with radiation set to 20 – 180 % of the mean values, while all the

other parameters were kept constant. The influence of this parameter on the mean surface temperature during the simulation period (16 hours) can be found in Figure 6.
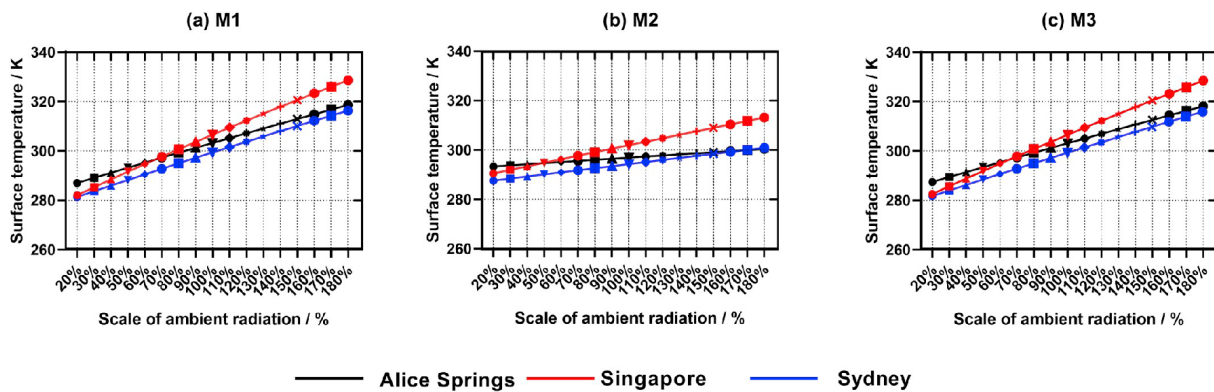

Figure 6: Three PDRC materials' sensitivity to changes in downwelling longwave radiation (DLR - here labelled as ambient radiation) in three distinct climates [50], considering the mean (100%) values of DLR for the climates: 348 W m^{-2} for Alice Springs, 365 W m^{-2} for Sidney and 418 W m^{-2} for Singapore.

Results show that higher levels of DLR result in a significant increase of the surface temperature of the material, which can lower the cooling effect and must be therefore considered when modelling the cooling performance of PDRC systems. The same sensitivity study was performed also for solar radiation, although all three materials considered were either ideal cases or extremely good solar reflectors (reflectance ≈ 0.99), so that the influence of solar radiation on cooling performance was less significant. Nonetheless, under peak solar radiation conditions close to 1000 W m^{-2} in Sydney and Alice Springs, one should consider that each 1 % reduction of solar reflectivity corresponds to a 10 W m^{-2} decrease in the surface cooling power.

Considering the mean solar radiation values in the cities (338 W m^{-2} in Alice Springs, 206 W m^{-2} in Singapore and 327 W m^{-2} in Sidney), Figure 6 makes it clear that even with low solar radiation, Singapore's tropical climate is inappropriate for the PDRC performance with the considered materials due to high downwelling longwave radiation. In contrast, despite the high solar radiation and air temperature, desertic climate in Alice Springs gives better PDRC results thanks to the high transparency of the atmospheric window.

5.2   Total precipitable water content

The principle of PDRC is strongly dependent on the transmittance of the atmosphere, which can be influenced by many factors such as the content of ozone, carbon dioxide, carbon monoxide, etc. However, the most significant factor is represented by the content of water vapour in the atmosphere, which is related to air humidity. Figure 7 shows the modelled transmittance of the atmosphere for two values of water vapour content (expressed as *TWC* – total water content). It is clear that the atmospheric transparency enabling the cooling effect in PDRC applications is progressively lost with increasing water vapour in the atmospheric column. A second atmospheric window between 16 and 23 μm, which could in principle contribute to the performance of broadband PDRC materials, is also typically suppressed by the presence of even moderately low water vapour content.
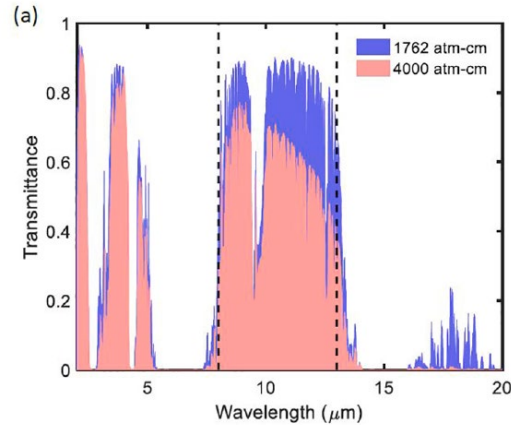
Figure 7: Modelled atmospheric transmittance with the conditions of typical cloud free summer day in US (total water content – TWC = 1762 atm-cm) and Shanghai (TWC = 4000 atm-cm) [51].

Liu *et al.* obtained both simulated and experimental results about the influence of water vapour content on the PDRC performance [51]. The dependence of the PDRC coating's cooling power on surface temperature T_s relative to the ambient temperature T_a for two values of water vapour content can be found in Figure 8. Both simulated (straight line) and experimental (dots and stars) data confirm the assumption that air humidity lowers the effectiveness of PDRC performance. For the smaller value of *TWC* (≈ 1000 atm-cm), experimental data measured in California correlate with the simulated line. In Hong Kong (*TWC* ≈ 4000 atm-cm), however, the measurements were strongly influenced by the cloud cover.
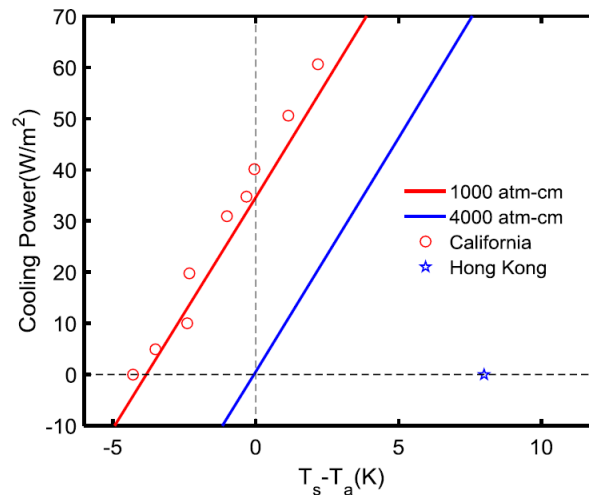

Figure 8: Modelled (straight line) and experimental (dots and stars) cooling power of a PDRC coating depending on the surface temperature T_s relative to the ambient temperature T_a, for two values of TWC (modelled non-radiative heat transfer coefficient h = 6.9 W m^{-2} K^{-1}) [51].

In an experimental report by Tso *et al.* [52], the cooling performance of a silicon substrate with a multilayer photonic structure in the humid Hong Kong climate was examined and compared with the dry weather conditions in California, where Raman *et al.* reported reaching a temperature drop of 4.9 °C below ambient air temperature under direct sunlight [5]. Due to the much larger total water content in Hong Kong, the same PDRC material failed to reach a temperature below ambient during the daytime and only succeeded in cooling during the night.

Similar negative effects of air humidity on PDRC effectivity was also reported by Yang *et al.* [53]. PDRC performance was simulated under weather conditions in five different cities in China and the effect of different total column water vapour (*TCWV*) values on PDRC is shown in Figure 9.
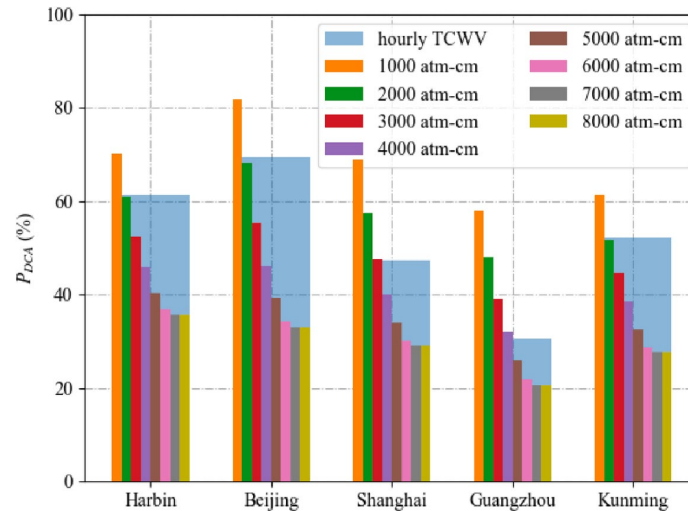
Figure 9: Effect of weather conditions in five cities in China and different values of total column water vapour (TCWV) on the annual percentage of the daytime hours during which the material can achieve sub-ambient cooling (P_{DCA}) for a simulated solar reflectance of 0.9 [53].

Besides the already-established lowering of PDRC performance by air humidity, Figure 9 also demonstrates that the relative decrease is strongest for lower values of *TCWV* (P_{DCA} decreases by 9.35 % when passing from 1000 atm-cm to 2000 atm-cm in Harbin), whereas the P_{DCA} drop eventually stabilises to a constant level for higher values of *TCWV* (0.22 % drop for a change from 7000 atm-cm to 8000 atm-cm in Harbin). Hence, the steepest drop in cooling performance is observed at low humidity levels, confirming that the applications of PDRC materials in tropical and wet climate areas remain limited.

Similar results have been reached by Aili *et al.* [54], where the dependence of relative humidity on a radiative and evaporative cooler was obtained both experimentally and numerically. Figure 10 shows the rise of the sub-ambient temperature with increasing relative humidity. The previously mentioned slowdown of the rising slope with higher humidity values is also visible. However, this data was measured for passive night-time radiative cooling, so the effect of solar radiation is neglected.

Huang *et al.* [55] computed the effect of air humidity on the atmospheric transmittance based on numerical simulation. When the ambient relative humidity increases from 20 % to 100 %, the peak of atmospheric transmittance in the 8 – 13 μm window falls from 90 % to 60 %, leading to a corresponding reduction of the PDRC efficacy. However, another influence is also discussed: air humidity contributes to higher aerosol scattering effect since aerosols are hygroscopic. This leads to a further reduction of atmospheric transmittance, but also of the solar radiation, which favours the PDRC effect. These opposite influences should be investigated in more depth to disambiguate some results reported in the literature. In fact, while most of the studies confirm the negative effect of humidity on PDRC performance, there are some reports of successful cooling performed even in moist climates. For example, Wang *et al.* [56] realised a temperature drop of 5.5 °C under solar radiation intensity of 930 W/m^2 and relative humidity of 64 % using a hierarchically structured PMMA film with a dense micropore monolayer array. This material exhibits a broadband emissivity in the IR range, which is typically considered detrimental under humid conditions based on the findings of other studies [57], in which broadband emitters are suggested for dry climate applications. The same material is also characterised by a broad angular emissivity, which is similarly unexpected since this factor should also lead to an enhanced radiative heat exchange with the atmosphere rather than outer space, and hence limit the overall sub-ambient PDRC potential.
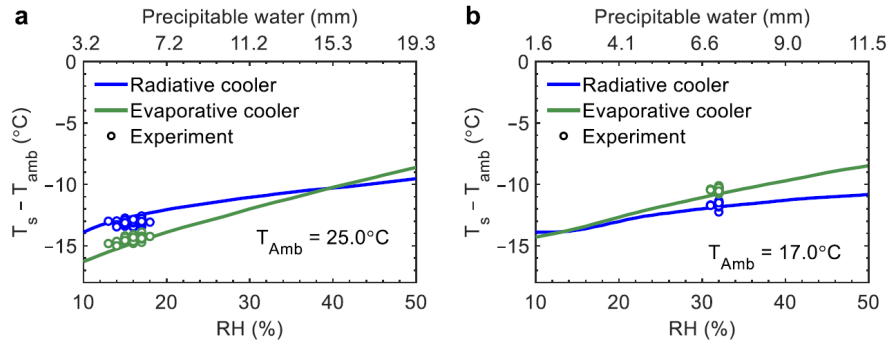
Figure 10: Effect of relative humidity on temperature drop of both radiative and evaporative coolers during night-time. Results are obtained both experimentally (dots) and numerically (lines) for two values of ambient temperature. The assumed wind velocities are 1.0 m/s and 0 for T_{amb} = 25 °C and 17 °C, respectively [54].

The effect of dew formation on the surface of radiative cooling materials is also directly related to air humidity. Spectral emittance of PDRC cooling materials can increase and broaden significantly in the presence of condensed water droplets, which can lead to a cooling performance limitation. Simsek *et al.* [58] measured spectral characteristics of various radiative coolers covered with acrylic droplets simulating water droplets and experimentally confirmed a negative effect of dew formation on cooling capacity. These experiments were held during the night, but water droplets forming on the surface of the coolers can also limit the cooling performance during daytime hours. Tao *et al.* reported that their proposed PDRC polymer-based material achieved better cooling results (2-3 °C larger temperature drop) with a hydrophobic surface modification [59]. For similar hydrophobic surfaces, a small tilt of the cooler could also be beneficial in a way that the condensed water can continuously flow away from the PDRC surface.

5.3   Cloud cover

Cloud cover is another of the climatic conditions that can impact heavily on the PRC performance both during night-time and daytime experiments. However, different levels of cloud cover, given by different types of clouds at different altitudes, can affect radiative cooling in many ways. On one hand, stronger cloud cover can reduce the radiative heat transfer between the PDRC coating and the sky, thus reducing the cooling effect. At the same time, scattered cloud cover can block solar irradiation, thus temporarily enhancing sub-ambient cooling. The thickness and altitude of clouds also plays a role of course, with thin, high-altitude cirrus clouds typically blocking less solar irradiation than thicker or lower-altitude cumulus clouds. Furthermore, certain high altitude clouds, made entirely by ice crystals, may still act as a heat sink for upwelling radiation, allowing some PRC effect despite veiled sky access [55].

In a theoretical study by Mokhtari *et al.* [60], an artificial neural network based on experimental results from four different measurements was used to predict the effect of cloud cover on PDRC function. The results confirm the correlation between higher cloud cover, and lower cooling performance. However, authors of the study highlight that this effect doesn't change linearly and no analytical predictions for the system performance were established.
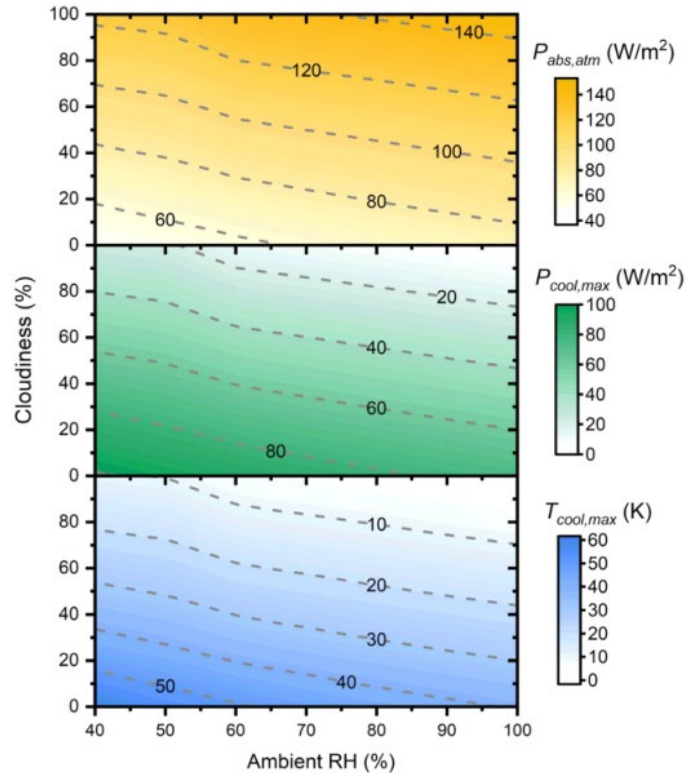
Figure 11: Numerically obtained values of radiation absorbed by atmosphere ($P_{abs,atm}$), maximum cooling power ($P_{cool,max}$) and maximum cooling temperature drop ($T_{cool,max}$) by an ideal PDRC material (narrowband emissivity of 1 in the 8 - 13 µm window, T_{amb} = 300 K) as a function of cloudiness and ambient relative humidity [55].

The correlation between cloud dover and PDRC performance has been also studied by Huang *et al.* [55], who proposed equations to obtain the amount of radiation absorbed both by clouds and atmosphere below clouds. Statistically, cloud cover fraction is approximately proportional to ambient relative humidity (when exceeding a critical value and thus forming clouds), but real-time cloud cover fraction has a weak correlation with humidity because it is affected by the overall meteorological-geographic status at a given moment. This fact makes simulating and predicting the effect of cloud cover on PDRC a difficult task. Figure 11 shows the amount of absorbed radiation, maximum cooling power and maximum cooling temperature drop of an ideal cooler as a function of cloudiness and ambient relative humidity. The results of this simulation agree on the PDRC performance reduction by clouds. Even for 100% cloudiness, the ideal cooler is in principle still capable of exerting a net cooling effect, which however eventually vanishes when the relative humidity value increases towards 100 %.

Yang *et al.* [53] also compared data obtained by numerical simulation of PDRC performance for clear-sky and cloudy conditions. Without clouds, the expected monotonic enhancement of the cooling performance with increasing solar reflectance is found for both selective and broadband emitters. When accounting in the model for the annual average cloud cover over a certain region, however, the authors suggest that broadband emitters may respond in opposite ways to an increase of their solar reflectance beyond 90 %, depending on different average cloud cover levels. These examples show that the effect of cloud cover on PDRC is complex, and it is yet to be fully understood by future research.

5.4   Non-radiative heat exchange

In the net cooling power equation (Equation 3), P_{nonrad} indicates the non-radiative heat exchange between the cooler and the ambient environment. This exchange term works as an inhibitor of the cooling efficiency as soon as the emitter reaches sub-ambient temperatures. Therefore, theoretically determined values of expected

cooling power of the systems obtained by ignoring these terms are difficult to observe in real conditions, and many of the experimentally tested PDRC materials are underperforming [31].

Non-radiative heat exchange is often described by the non-radiative heat exchange coefficient (*NRHEC*, h_C). The effect of this coefficient on PDRC is crucial. As calculated by Chen *et al.* [61], in the absence of *NRHEC* (h_C = 0 W m^{-2} K^{-1}), an ideal emitter could theoretically reach temperature drops of 50 °C below ambient. At more realistic values of h_C = 8 W m^{-2} K^{-1}, however, the maximum attainable drop decreases to 10 °C only. The key role of non-radiative heat exchange channels was also confirmed experimentally by the same authors, by placing the PDRC into a sun-shaded vacuum chamber with a IR-transparent window on top. A maximum temperature reduction of 42 °C below ambient was measured by this system. Additional strategies to reduce the *NRHEC* include the use of heavy gases such as krypton for the sample enclosure [48], using IR-transparent polyethylene films or aerogel layers to insulate the emitter from external air [62]. Alternatively, Qin *et al.* [63] recently proposed to suspend the passive radiative cooling system in a completely open environment, since a large part of non-radiative heat exchange is realised by convection inside sealed systems. However, both vacuum and open environment systems add significant challenges for the majority of practical PDRC applications.

NRHEC directly correlates with wind speed, which makes it one of the main parameters that is studied in relation to the magnitude of non-radiative heat transfer. The correlation is mostly believed to be linear ($h_C = a + bv$, where v is the wind speed and a and b are the empirical constants determined by experimental or theoretical methods). However, to suppress the negative effect of the wind on PDRC performance, various types of cover shields were applied to the PDRC setup. Cover shields are designed to be infrared-transparent and convection-suppressive, while they can be either transparent or opaque in a visible spectrum. With the use of an effectively-designed cover shield, the linear dependence of *NRHEC* on the wind speed can be suppressed, allowing to stabilise the value of *NRHEC* [31].

Figure 12 includes both ambient conditions and PDRC material temperatures for an experiment conducted on a clear and breezy day by Jiu *et al.* [64]. Blue and red lines in Figure 12b show the temperatures of the radiative cooler without and with the wind cover, respectively. Although the performance of the cooler with wind cover is visibly better, the direct influence of the wind speed (grey line) is unclear due to the combined variability of all other environmental parameters (solar irradiation, relative humidity, ambient temperature).

It should be noted that *NRHEC* is frequently neglected in many studies on PDRC performances. One of the most used figures-of-merit, i.e., the cooling power measured with the sample kept at ambient temperature, should in fact suppress non-radiative contributions since both the sample and the environment are kept at the same temperature. This topic will be further discussed in subsection 6.1.3.
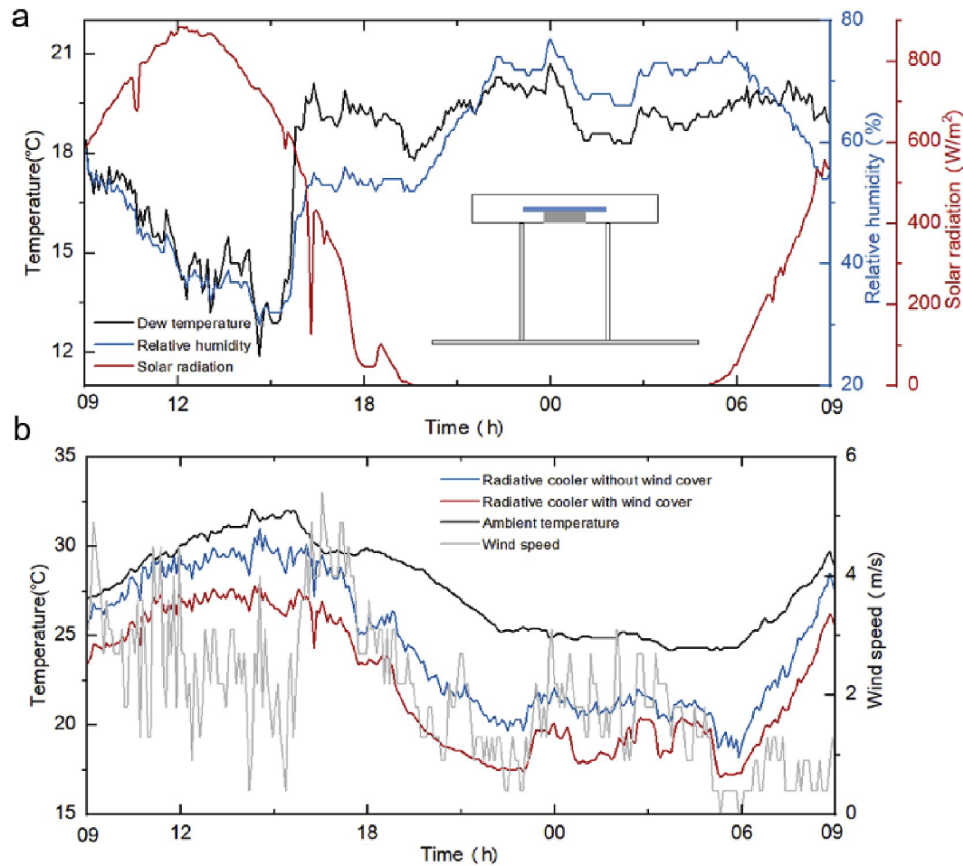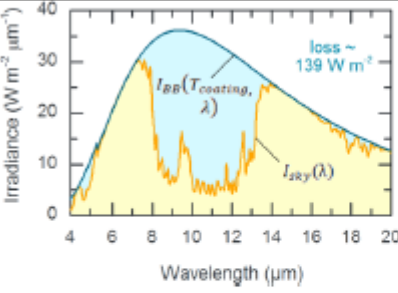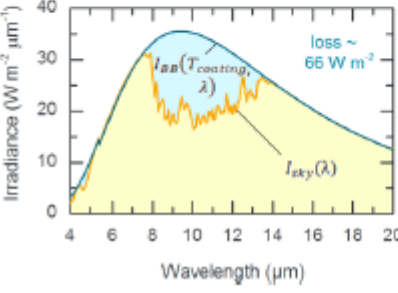
Figure 12: PDRC performance in a 24-hour experiment on a clear and breezy day [64].

5.5   Geoclimatic conditions

On average, atmospheric conditions are related to the geoclimatic conditions of a location. Solar and ambient radiation, air humidity, ambient temperature and weather of the location must be all taken into account when trying to predict the cooling potential in a given place. Some of the studies comparing PDRC performance in different geoclimatic locations were already presented [50, 52-53]. In addition to the mentioned parameters, Mandal *et al.* reports other influencing factors such as higher solar elevation angles, lower surface temperatures, lower elevations (i.e. thicker atmospheres) and higher aerosol contents, which can lead to a decline in PDRC effectivity [42]. Consequently, subtropical and humid locations with low latitudes are less suitable for PDRC applications than mid-latitude, arid and elevated locations (Table 1).

Table 1: Comparison of estimated cooling performance in Southwest USA and South Asia based on experimental measurements [42].


Similarly, Liu *et al.* [64-65] computed theoretical PDRC potential in China finding comparable results (Figure 13) – cooling potential (expressed as cooling power values in Fig. 13a and temperature drop in Fig. 13b) rises approximately from southeast to northwest, with higher latitudes as well as with longer distance from sea. In Fig. 13b, areas located in the southeast region even have negative PDRC potential. That is due to the temperature of the radiative cooler being higher than the ambient temperature and wind cover blocking the non-radiative heat transfer with the environment.

Furthermore, Yu *et al.* predicted the PDRC potential in six different standard model atmospheres available in the MODTRAN application [66]. The summary of the differences between the atmospheres is given in Table 2.

Table 2: Parameters of six different standard model atmospheres used in [66].

model	water column (atm-cm)	ozone column (atm-cm)	ground atmosphere (K)
tropical	5119.4	0.27727	299.7
mid-latitude summer	1059.7	0.37681	272.2
mid-latitude winter	2589.4	0.34492	287.2
sub-arctic summer	2589.4	0.34492	287.2
sub-arctic winter	517.73	0.3755	257.2
U.S. standard 1976	1762.3	0.34356	288.15

(a)
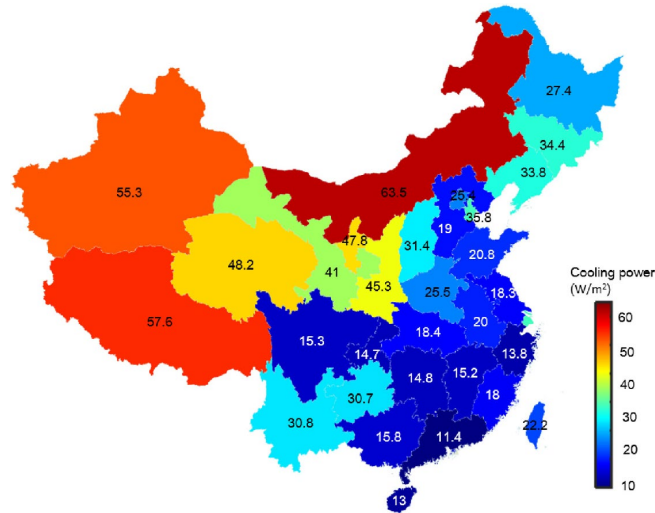
(b)
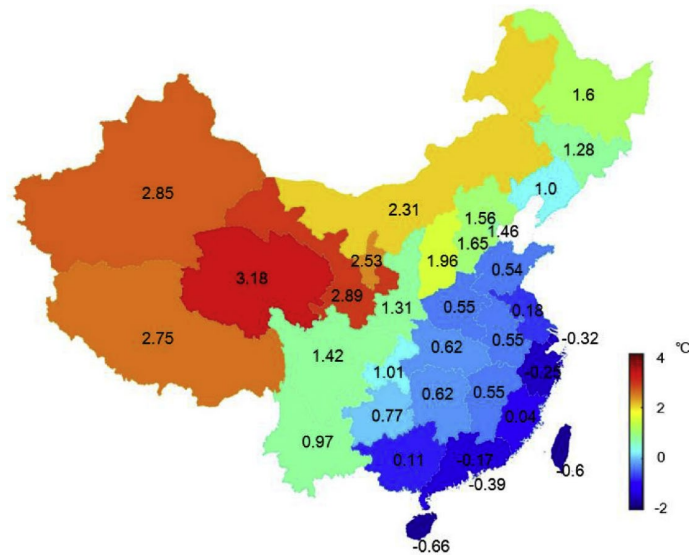
Figure 13: Theoretical cooling potential of a PDRC material in different areas in China, (a) expressed in cooling power (W m⁻²) [65], (b) expressed in temperature drop (°C) using a wind cover to suppress non-radiative heat transfer [64].

Figure 14 shows the results of the simulation (standard model) and of two experimental measurements (experimental model) taken from [42]. As it can be seen, total water column (y axis) and ground temperature (x axis) have competing effects on the estimated cooling power. For both high water column and low temperature, cooling power is low, and best results for standard models were obtained approximately at intermediate conditions (US standard 1976). However, both experimental models are placed outside the standard model range and the measured cooling power is larger. This result suggests that commonly used standard atmospheric models may not provide sufficient information to correctly predict the expected PDRC performance.
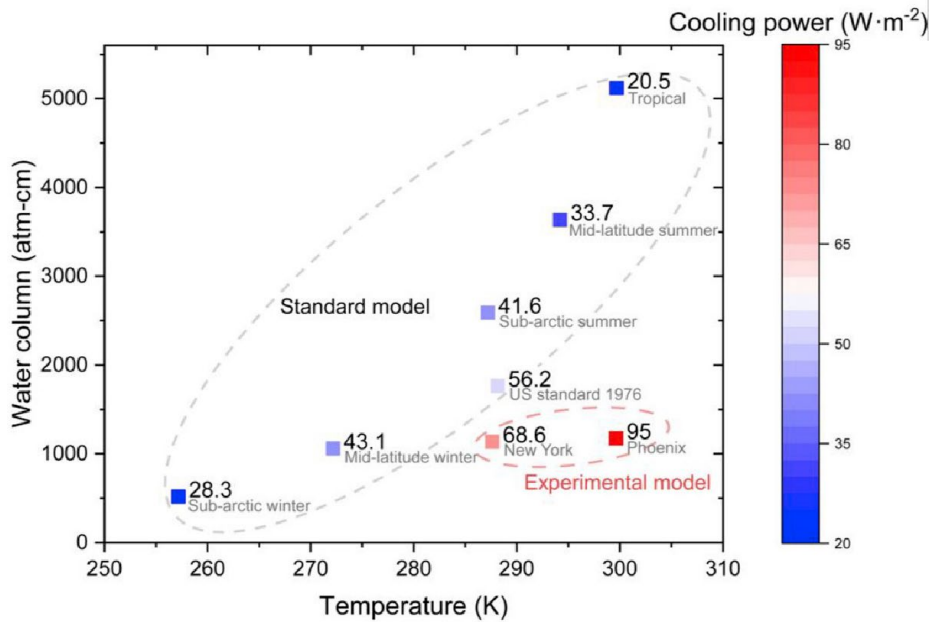
Figure 14: Estimated cooling power in six different standard atmosphere models accompanied by results of two experimental models [66].

Huang, et al. [55], performed similar numerical predictions for a worldwide prospect of cooling performance. Their calculation was based on data from 240 cities around the world, including monthly temperature, humidity, wind, cloud cover fraction and seasonal aerosol. Their findings, shown in Figure 15, are in line with the already mentioned studies - low humidity, cloud coverage and wind speed contribute to higher cooling powers. The Arabian Peninsula, Western United States, Northern Africa and Western Australia were marked as locations with the highest potential for PDRC applications.
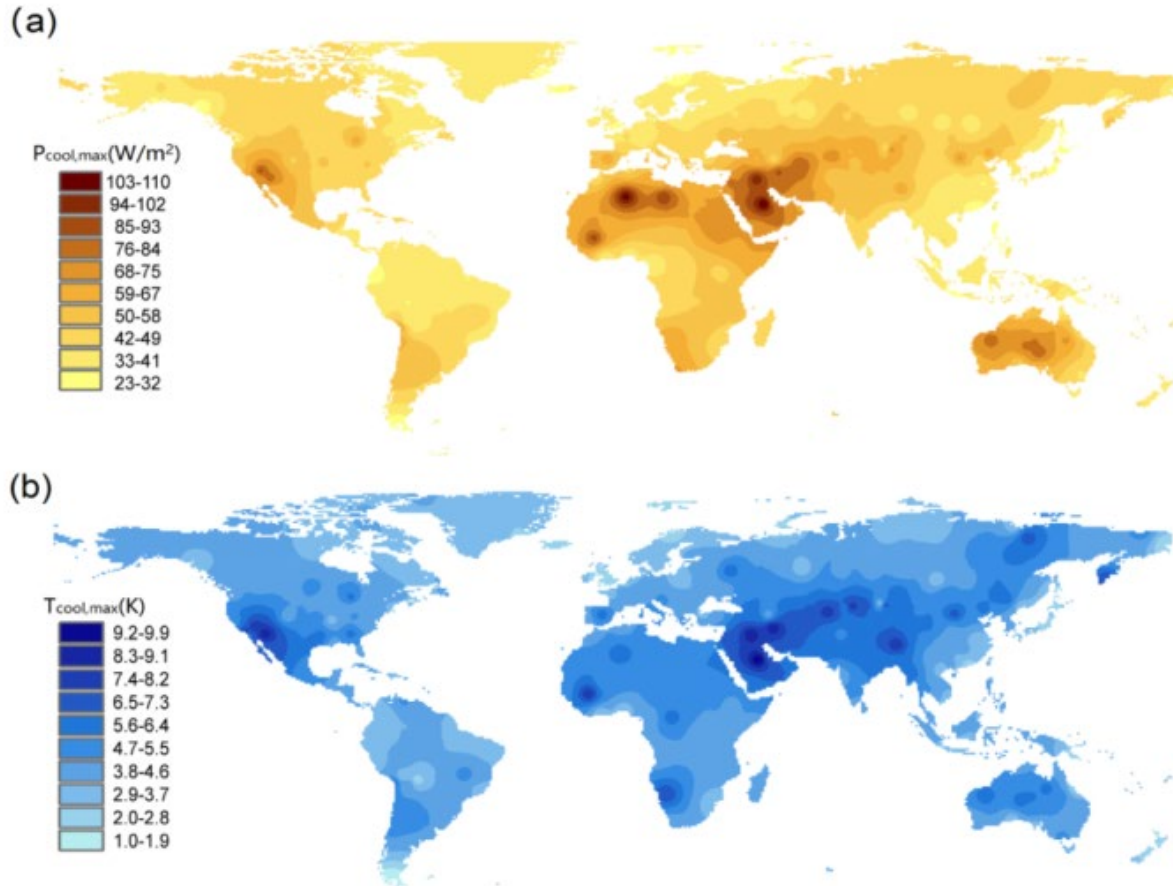
Figure 15: Maximum cooling power and maximum temperature drop of a PDRC system worldwide based on geoclimatic data [55].

Dedicated studies on both the daytime and night-time radiative cooling potential in the European region have been conducted by Vilà et al. [67] for different hypothetical values of solar reflectivity, based on weather data from a database of weather stations across several countries. Their results show that the climatic conditions found in southern Spain, Greece and Turkey are most favourable for all-day radiative cooling (Figure 16). Notably, the same group confirmed that comparable radiative cooling potentials can be expected also in consideration of future climatic scenarios, by taking into account the expected evolution of changing geoclimatic scenarios in Europe up to 2050 [68].
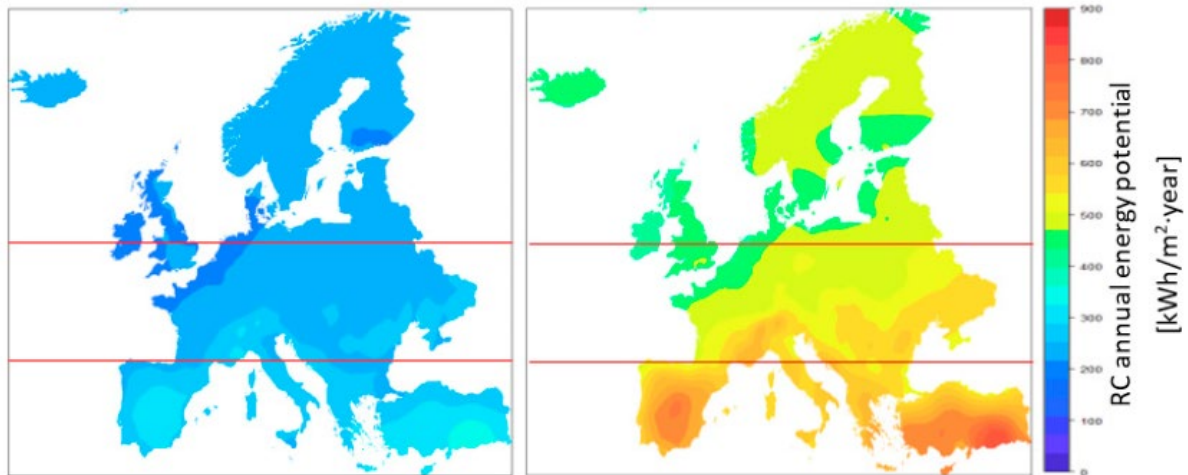
Figure 16: Map of radiative cooling annual energy potential in Europe for night-time (left) and all-day use (right). Computed for the ideal solar radiation reflectivity $\rho = 1$ [67].

Finally, Lin *et al.* also discussed how PDRC materials should be designed to have different properties depending on their target location [57]. The authors suggest that for hot and humid areas, the only residual atmospheric transmittance available is in the wavelength region from 8 to 13 µm. Thus, selective radiative coolers with high emissivity in this region are suitable for effective PDRC. However, in cold and dry areas, the atmospheric transmittance is higher across a broader wavelength range, and broadband emitters may become preferable. Different conclusions were reached however in a study by Feng *et al.* [50], showing that selective emitters should reach lower cooling temperatures than broadband emitters in a wide range of ambient conditions. Desirable emissivity spectrums are discussed in detail in subsection 6.1.1.

5.6   Thickness

Herrmann *et al.* published a study on the identification of the optimal thickness for a PDRC coating [69]. They used a PDRC configuration based on transparent, unpatterned polydimethylsiloxane and calculated the cooling power from its complex refractive index data. Figure 17 shows the dependence of coating thickness on individual energetic components as well as cooling power.
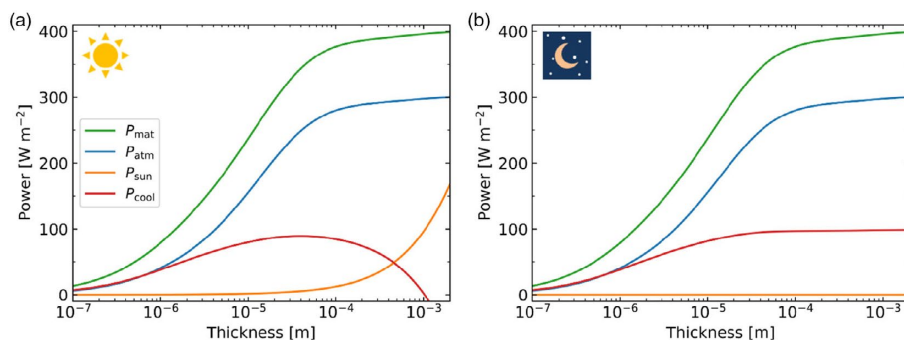
Figure 17: Individual energetic components at ambient temperatures as a function of thickness for (a) daytime and (b) night-time cooling, as well as the resulting cooling power [69].

Results show that for daytime cooling (Figure 17a), maximum cooling power can be found for a specific thickness value and for higher values, the low but finite absorption of solar radiation eventually lowers the resulting cooling power. For night-time cooling (Figure 17b), on the other hand, optimum thickness is rather a factor for minimising fabrication costs.

Analogue considerations hold also for defining the most suitable thickness in the case of diffuse reflectors. For an ideal diffuser, transmittance is expected to decrease with the inverse of the thickness (a principle sometimes

referred to as Ohm's law for light). In reality, however, due to the inevitable presence of some spurious absorption, transmittance is eventually suppressed exponentially, with no net gain in reflectivity beyond a certain thickness. For this reason, increasing thickness is typically associated with diminishing returns in terms of reflectivity, as shown for instance in Figure 18. This effect makes the choice of the best thickness value for a PDRC material strongly dependent on fabrication cost and applicability in real systems. In the case of PDRC paints, the optimal thickness is typically defined as the minimum thickness sufficient to obtain a substrate-independent reflectivity, with higher thickness values leading to higher costs and potentially problematic paint weight per unit area. Thickness values reported in the literature are therefore all typically around a common value of ~500 µm. For example, when characterising scalable aqueous-based PDRC paint introduced in [70], a thickness of 460-610 µm was recommended, even though research efforts are directed towards lowering this value, for instance by using nanoplatelet scatterers [71]. In fact, keeping the absolute thickness of paint-like PDRC materials low may be relevant to drain heat efficiently from the coated substrate.
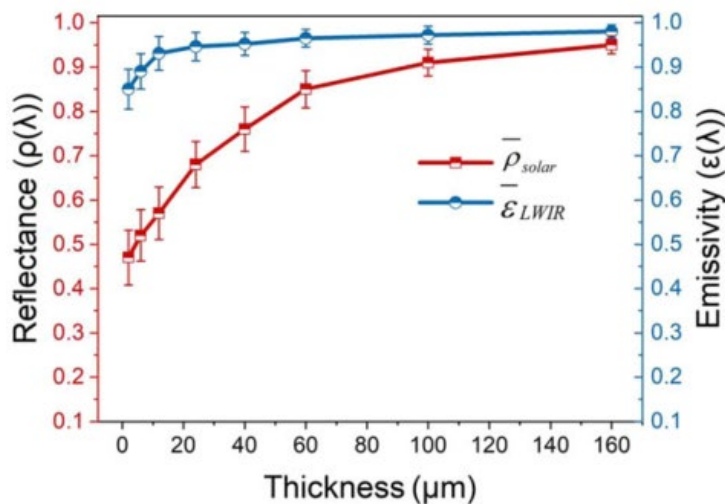
Figure 18: Solar reflectance and emissivity in a 8 - 13 µm window of a PMMA-based emitter used in [56] as a function of layer thickness.

5.7 Angle of radiation

The zenith angle of the PDRC coating contributes to the effectiveness of the cooling, mainly at lower ambient temperatures. Jeon *et al.* conducted a theoretical study considering different zenith angles for selective and broadband emitters [72]. They reported that at ambient temperature, both types of emitters exhibited non-negative net radiance at all zenith angles. However, below-ambient temperatures, the radiative contributions become detrimental at large zenith angles. The authors explain this behaviour in terms of the gradual increase of the atmospheric radiance at higher zenith angles and the gradual decrease of the blackbody radiance at lower temperatures. A summary of the results is shown in Figure 19.
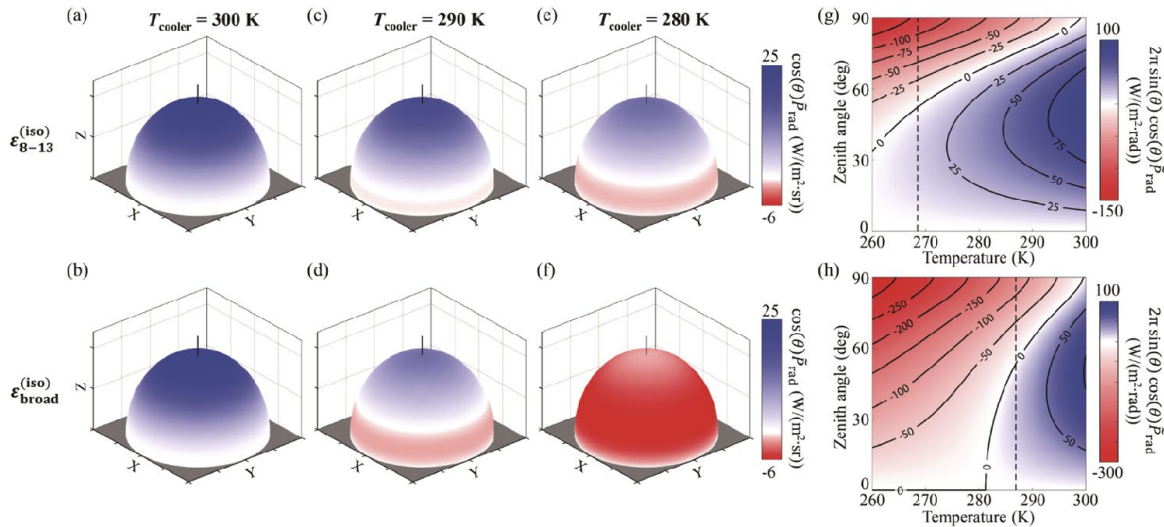
Figure 19: Cooling performance of a selective emitter (upper row) and a broadband emitter (bottom row) at different zenith angles and temperatures [72].

For lower temperatures (280 K), broadband emitters work as a heater instead of cooler at all zenith angles. For selective emitters, cooling works for low zenith angles, high values also lead to heating instead of cooling. Dashed lines in Figures 19g and 19h show the values of steady-state temperatures (zero radiative power density), which is significantly lower in the case of selective emitters.

It is interesting to comment on these calculations with respect to the previously mentioned experimental measurement of Wang *et al.* [56], where a broadband emitter with very high emissivity also at large angles (Figure 20) was used to obtain a remarkable cooling result (5.5 °C temperature drop under direct solar irradiation). The experiment described by Wang *et al.* was performed at temperatures slightly above 300 K, where all angles can in principle contribute some net cooling power even in the case of broadband emitters. As discussed previously, emissivity at high angles could be beneficial due to a thermal exchange between the emitter and some parts of a humid atmosphere. Other studies should be performed to confirm the positive effect of broadband and angular emissivity on PDRC performance in humid conditions.
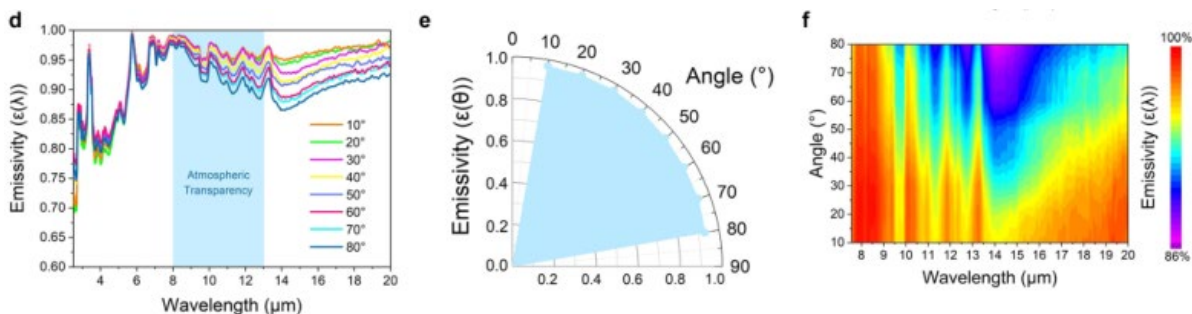
Figure 20: Characterization of a PMMA-based emitter used in [56] - broadband and angular emissivity.

Another important aspect to consider for the performance of PDRC materials, is their relative tilting with respect to the sky and surrounding environment. Due to their high emissivity, PDRC materials should be preferably directed towards the zenith direction, where the atmosphere thickness is lowest, along with its downwelling irradiance. Tilting the PDRC sample would expose it to a larger thermal irradiance from the sky and, above a certain angle, even from the thermal glow from nearby buildings and obstacles, or the thermal "glow" from the ground itself. However, different considerations hold with respect to solar heat gains. Even a moderate back-to-sun tilting is in fact known to enhance considerably the observed PDRC effect due to the correspondingly lower solar irradiance received by the emitter [73-74].

In the scientific literature, several PDRC materials are often placed horizontally during the tests, or even facing the sun directly to provide a more compelling demonstration of their performance under adverse conditions. However, in practical applications, sky-cooling panels providing cold water will be likely oriented slightly away from the sun, to enhance their performance. Either in the form of panels or super-cool roofs, PDRC materials are sometimes seen as competing for roof space with other technologies such as photovoltaic or solar thermal panels. In practice, this is extremely unlikely since their ideal placement requires diametrically opposed orientations. The best trade-off between a tilting angle to enhance daytime cooling without excessively penalising night-time cooling will depend on the exact location and angular dependence of the PDRC material emissivity.

5.8 Concentrated PDRC and reciprocity

System reciprocity is an important constraint that must be taken into account for PDRC applications. The symmetry of radiative transmission received and emitted by the system limits the cooling performance that can be achieved. The topic of reciprocity is often studied in relation to concentrated radiative cooling, which is a way to enhance the PDRC effect. As solar irradiation is one of the main sources of cooling performance loss, mirrors with various configurations and spectral selectivity are used to keep cooling ability even without directly facing the sky. Two examples of this approach are illustrated in Figure 21. In Figure 21a [75], two tilted mirrors are used to absorb solar irradiance before it can reach the PDRC material, while simultaneously reflecting the thermal radiation coming both to and from the emitter. In Figures 21b and 21c [7], a similar concentrated geometry is used for the cooling process of a fluid in a system of pipes.
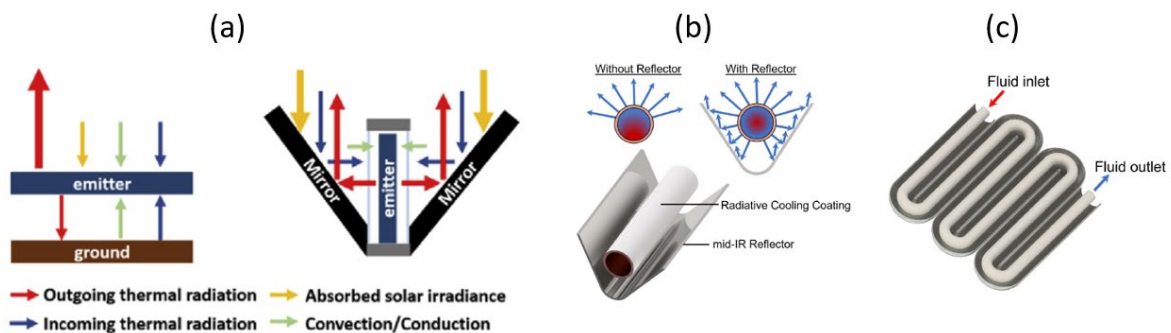
Figure 21: (a) Geometry of a concentrated radiative cooling system [75], (b) design of concentrated radiative liquid cooling system [7], (c) implementation of liquid cooling to a larger scale [7].

When modelling these systems, it is however important to correctly account for reciprocity. Concentrators can shield part of the thermal radiation from the atmosphere, but will also redirect some of it towards the emitter. In this respect, the funnelling principle of a concentrator relies on the fact that the downwelling atmospheric irradiance is not isotropic. Dong *et al.* pointed out that in many recent studies suggesting a concentrated PDRC performance of novel materials, the estimated cooling power is overestimated due to an incorrect account of reciprocal radiative heat gains [76]. Omitting reciprocity considerations during numerical studies can incorrectly lead to better cooling performances of the materials, which are in fact non physical.

Concentrating configurations can in principle facilitate the observation of a measurable cooling power using smaller samples and testing setups. However, the need to fully characterize the properties of concentrating mirrors would introduce an additional source of uncertainty on the measured figures of merit. Therefore, the use of concentrating configurations will not be considered within the scope of the PaRaMetriC project.

6 Figures of merit and comparison methods

An increasing number of passive daytime radiative cooling materials and applications is reported and tested each year. Significant progress happening in the field of PDRC in recent years also creates higher demand for reliable and universal methods for comparing the performance of novel materials and predicting their cooling abilities in different environments. However, widely agreed methods have not been identified or validated yet. Bu *et al.* defines three main obstacles that result in inconsistencies in the measured data comparisons [77]: i) different measurement standards, ii) different experimental setups and iii) reporting different figures of merit for measured data. Figures of merit used in the majority of published studies are strongly dependent on both the experimental conditions and thermal properties of the materials, resulting in the impossibility of comparing the performance of different materials directly against each other in a consistent way. In the following sections, frequently used figures of merit for PDRC materials will be described, then some more specific, cooling performance-based parameters will be discussed and previous studies dealing with this problem will be presented.

6.1 Frequently used PDRC parameters

6.1.1 Emissivity spectrum

Considering the basics of PDRC, the spectral properties of the material are often used to characterise its suitability for these applications. The emissivity spectrum of the material has to be measured and its similarity with the ideal emitter models is then evaluated. Among several possible definitions of idealised emissivity spectra [78-79], two options are most commonly used for designing PDRC materials: narrow-band emitter with high emissivity within 8 – 13 µm, and broadband emitter with high emissivity within 4 – 25 µm. In both cases, the materials should have zero emissivity in the solar spectrum. These two types of materials present specific advantages in different working conditions. Broadband emitters are able to radiate more heat outward, hence reaching potentially higher cooling powers, but only at a temperature above or slightly below the ambient. On the other hand, narrow-band emitters are suitable to realise larger sub-ambient temperature drops as their cooling power decreases more slowly with decreasing temperatures, and they are more radiatively insulated from atmospheric irradiance. Narrow-band emitters are therefore able to reach lower cooling temperature in absolute terms than broadband emitters [80]. However, as previously discussed in subsection 5.5, broadband emitters can still be used for sub-ambient cooling, mostly in cold and dry areas with high atmospheric transmittance.

Other ideal emissivity profiles have also been proposed, for example by Xu *et al.* [78], where the authors suggested an alternative selective profile with an emissivity drop between 9 and 10 µm to avoid radiative exchanges with the ozone absorption band in that wavelength range. However, such fine tailoring of the emissivity profile is difficult to achieve in actual samples. Jeon *et al.* [81] came to similar conclusions in their theoretical work on the ideal emissivity spectrum for PDRC materials. Figure 22 shows the ideal emissivity windows as a function of non-radiative heat transfer coefficient h_C. An additional drop between 9 and 10 µm can be seen, as well as a narrowing of the ideal window as non-radiative losses are progressively reduced towards $h_C = 0$ W m^{-2} K^{-1}.
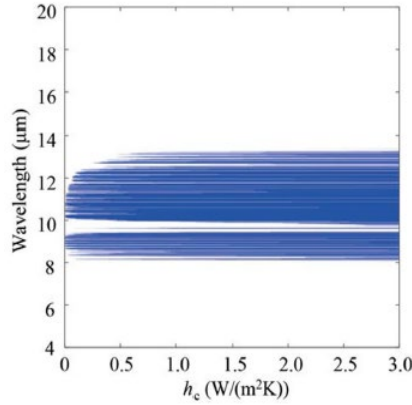
Figure 22: Ideal emissivity spectrum of PDRC materials for different values of non-radiative heat transfer coefficient (h_C) [81].

Numeric analysis of different emissivity profiles and PDRC performance of the emitters can be also found in the work of Kecebas *et al.* [82]. According to their simulations, the ideal emissivity for reaching the lowest equilibrium temperature depends on a total heat load *q* acting on the surface from both radiative and non-radiative contributions. In the case of nearly insulated systems, values of *q* approach zero and lowest temperatures are reached when the emissivity is narrowed between 10 – 12 µm. However, with increasing q, the ideal emissivity broadens first to the usual narrow-band (8 – 13 µm) profile, and eventually to the broadband case (> 8 µm). Figure 23 shows the transition points from narrow-band to broadband emitters, as defined by the critical power P_{crit} where the lowest equilibrium temperatures reached by selective and broadband emitters become equal. The transition is related to the narrow-band emitter not being able to compensate for the total heat load at a given temperature compared to the broadband emitter. For $q < P_{\text{crit}}$, narrow-band (selective) emitters reach lower equilibrium temperature, whereas broadband emitters are more efficient for $q < P_{\text{crit}}$. In Figure 23a, P_{crit} increases with rising ambient temperature T_{amb}, which suggests that even though broadband emitters are believed to reach higher cooling power at higher temperatures, as previously mentioned, narrow-band emitters are still capable of reaching lower equilibrium temperature. However, Figure 23b shows that with increasing non-radiative heat transfer h_C, the difference between the different types of emitters becomes negligible. Near-total insulation conditions with h_C close to zero are almost impossible to obtain under real-life conditions, therefore, according to the study of Kecebas *et al.*, additional studies on tailored broadband emitters represent a promising direction for the further advancement of the field.

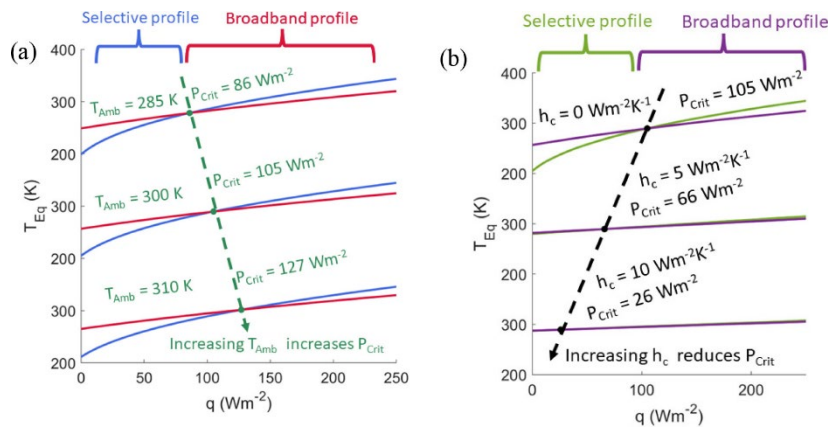*Figure 23: Comparison of narrow-band (8 – 13 µm) and broadband (> 8 µm) emitters and their ability to reach lowest equilibrium temperature, pictured as a function of a total heat load q acting on the PDRC surface. (a) Fixed value of non-radiative heat transfer coefficient h_C = 0 W m^{-2} K^{-1}, increasing ambient temperature T_{amb}, (b) Fixed T_{amb} = 297 K, increasing h_C [82].*

Numeric-simulation studies use mostly emitters with ideal parameters ($\varepsilon = 0$ or 1, considering the actual model), whereas real emitters have emissivity values in the wavelength range of interest around >0.8 in most cases. The suitability of a material for PDRC applications can be intuitively guessed from its emissivity spectrum, even though there are obviously more factors at play. Besides the emissivity spectrum, other spectral descriptors can be found in the literature. Infrared radiance of the material carries similar information as emissivity, however it expresses the actual amount of radiation emitted by an object in a particular direction, which however requires the use of dedicated equipment which may not be available to end users. IR radiance measurements can be used as a reference method against which typical emissivity data can be compared. Moreover, its capability of retrieving wavelength and angular resolved data is key for the characterisation of PDRC materials due to the importance of their angular response compared to their orientation with the atmosphere, and to the possibility of retrieving directly the hemispherical emissivity, which is the relevant quantity for heat balance calculations. For some applications, such as the research on transparent PDRC windows, transmittance is also a valuable parameter. Chowdhary *et al.* use visible transmittance (*VT*) and infrared transmittance (*IRT*), which represent the portion of visible and infrared radiation transmitted through a glass window over a particular wavelength range, respectively [83]. The calculation of the contrast ratio (*CR = VT/IRT*) determines the ability of the PDRC glass to simultaneously achieve maximum transmission in the visible regime and minimum transmission in the IR regime, therefore higher *CR* values indicate better material performance for this application.

6.1.2 Solar reflectance

Besides emissivity, solar reflectance is another parameter strongly correlated with PDRC performance. As suggested by Bu *et al.*, however, optical characterization and solar reflectivity measurements are often affected by common shortcomings in several recent studies on PDRC materials [77]. In ultraviolet-visible-near-infrared spectroscopy, standard reference samples are often measured prior to the actual cooling material measurement, for calibration purposes. Unfortunately, most studies do not specify whether the reported reflectance values are absolute or relative to the reference standard. The reflectance of the standards is typically below 100 %, even within the specification of the manufacturers, which can lead to a significant reflectance overestimation if only relative values are reported. Figure 24 shows the difference between relative and absolute values of reflectivity compared by Bu *et al.* The approximation of the reflectivity of reference samples can lead to a critical 25 % underestimation of the overall solar absorption, introducing a systematic bias which affects the cooling performance.
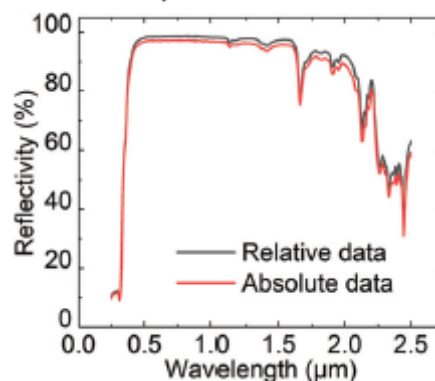
Figure 24: Relative reflectivity (acquired by UV-vis-NIR spectrometer PerkinElmer Lambda 950) compared to absolute reflectivity computed from the spectral reflectivity of the manufacturer-provided reference standard [77].

Bu *et al.* also stresses the fact that optical properties measurement uncertainty can cause significant errors in cooling efficiency prediction. It is therefore important to include uncertainty estimation when presenting PDRC materials characterization.

6.1.3 Cooling power

Cooling power P_{net} (W m^{-2}) is often reported as a determining result of a PDRC measurement or simulation. It can be calculated using Equation 3, its accuracy however depends critically on the ability to correctly measure all contributing terms. When said contributions are approximated or neglected, the resulting P_{net} value might be misleading. Additionally, looking at Equation 3, it is clear that the final cooling power result depends not only on the spectral properties of the material, but also on the experimental testing conditions and the other factors affecting PDRC performance as described in previous sections. Therefore, when comparing various PDRC materials, it is not possible to rely solely on its cooling power as this quantity is largely dependent on the measurement conditions. Also, it should be noted that based on Equation 3, an upper limit value for the cooling power attainable by an ideal PDRC material under ideal conditions can in principle be estimated, which is typically reported at around 150 W m^{-2} [84].

For the experimental measurement of this quantity, Raman *et al.* [5] proposed a method to obtain P_{net} by heating a PDRC material using an external electric heating pad. Cooling power is then determined as the electric power dissipated by the heater when the temperature of the PDRC material equals the ambient temperature of the environment. Figure 25 illustrates the cooling power measurement. As it can be seen, among other effects, the cooling power value is directly connected to the value of solar irradiance during the experiment.
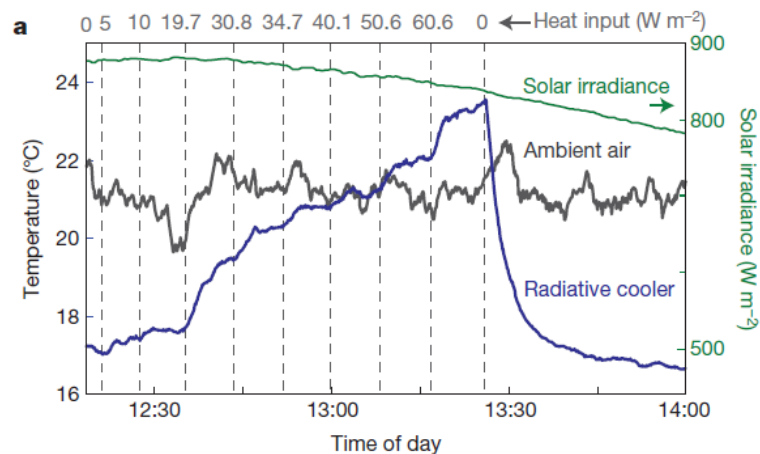
Figure 25: Experimental determination of the cooling power of the PDRC material. Cooling power is taken from the heat input value for the point where cooler temperature (blue line) equals ambient air temperature (black line) [5].

To measure cooling power of a PDRC coating in real time, a feedback-controlled loop can be added to continuously tune the current flowing through the electric heater in such a way that the temperature of the coating under test matches that of the ambient air at all times. Figure 26 shows an online measurement of cooling power in an outdoor setup by Qin *et al.* [63]. It is clear that the value of the cooling power is correlated with the temperature fluctuations and every time the temperature decreases, the measured cooling power also drops significantly. This indicates that among other influences such as wind speed and solar irradiance, the accumulation of the heat in the measuring box or at the coating surface can also significantly affect the resulting cooling power, which is often reported as an average value from the whole cooling experiment.
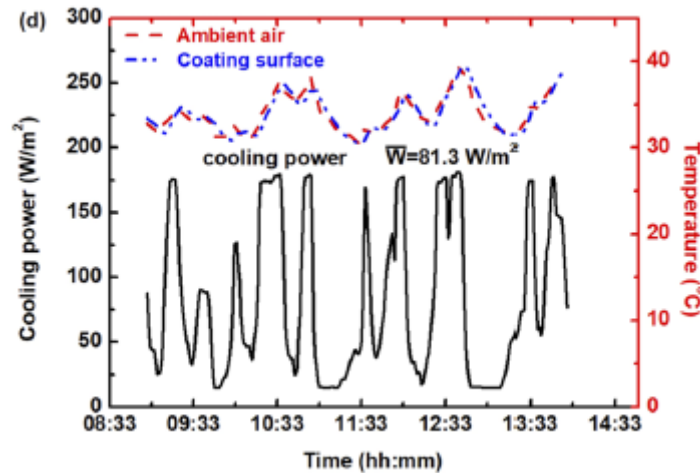
Figure 26: Online cooling power measurement obtained by maintaining temperatures of coating surface and of ambient air at the same values [63].

This experimental approach to measure the cooling power of PDRC materials has some disadvantages. When reporting the experimental data, most researchers assume that 100 % of the heat generated by the electric heater is transferred to the emitter and dissipated radiatively by it, i.e., assuming purely one-dimensional heat transfer from the heater to the cooled substrate. Not securing this condition can lead to significant cooling power overestimations and exaggerated cooling power claims. Possible solutions to this problem involve using more advanced heating systems, inspired by the guarded-hot-plate method, as applied by Leroy *et al.* [34, 62].

Alternatively, the cooling power could be estimated using a controlled water flux kept in thermal contact with the backside of the emitter, as first exemplified in the work of Goldstein *et al.* [12]. An advantage of this method is that the inlet and outlet water temperatures can be measured with high accuracy, as well as the instantaneous water flux. Moreover, the measured value would represent a conservative estimate, since any deviation from the ideal insulation of the system would result in an underestimation of the cooling power, rather than an overestimation.

6.1.4 Temperature

The most basic characterization used during PDRC experimental tests is a direct temperature measurement. Several thermocouples are often used to monitor the temperature of the PDRC material surface or the substrates cooled down by it (T_s), to be compared with ambient temperature (T_{amb}). Most of the studies provide the results by showing just the lowest achieved temperature or more commonly a temperature difference between T_s and T_{amb}. Alternatively, the maximum temperature drop (*MTD*) is sometimes reported [33]. The information about the temperature difference is beneficial for comparing various PDRC materials tested in similar working conditions or experiments with similar PDRC materials tested in various working conditions, but cannot be used for a more universal material comparison. Besides temperatures being strongly dependent on the experimental conditions, several shortcomings are also associated with the determination of T_{amb}, since its measurement depends critically on the placement of the thermocouple and its proper shielding from other external factors. Many of the exceptionally high temperature differences reported in the literature can probably be ascribed to significant overestimations of T_{amb}, obtained by either measuring it under direct solar radiation or with insufficient shielding from other radiative and convective heat sources. When reporting the obtained temperature difference as an indicator of PDRC performance, it is therefore crucial to ensure accurate T_{amb} measurement.

The term equilibrium temperature T_{eq} can also be used with different meanings in the literature. Some studies use this term to refer to temperatures obtained under different conditions and non-zero cooling power. It can be also used as a determining computed parameter. On the other hand, looking at Equation 3, P_{net} and P_{rad} depend on the temperature of the material surface T_s, whereas P_{atm} depends on the ambient temperature T_{amb}. T_{eq} is therefore equal to T_s when cooling power $P_{net}(T_s) = 0$. Reaching the equilibrium condition can lead to

T_{eq} being either lower or higher than T_{amb}. Ao *et al.* [85] considers the equilibrium temperature as a key parameter for PDRC performance, together with cooling power P_{net} at the ambient temperature T_{amb}. Working conditions of a PDRC material can be set either to reach the lowest equilibrium temperature T_{eq} or to obtain the highest cooling power P_{net} possible [86]. Zhao *et al.* [2] conducted field experiments where just the simple temperature difference was measured and the obtained data was then used to calculate equilibrium temperatures of other simulated emitters by thermal simulation (previously shown in Figure 5). Obtaining the equilibrium temperature can be useful for finding the right conditions to obtain a certain PDRC performance, but once again this quantity remains heavily dependent on other parameters and should be defined unequivocally to avoid confusion.

As a final remark, it should be noted that values of cooling power at ambient temperature and equilibrium temperature at $P_{net} = 0$ are typically presented as two alternative methods for the evaluation of the cooling performance of a PDRC material. However, their interpretation can be unified by considering them as two points on a single curve describing the dependence of the cooler temperature on the achieved cooling power. It is clear that to obtain a more comprehensive characterisation of the cooler, more points of this curve should be reported [87], since the performance of PDRC materials can depend on the temperature of the emitter. Measuring more data points on the curve is on the other hand problematic due to the time needed for the temperature stabilisation of each value, which can lead to changes in external conditions and therefore to a distortion of the data, unless multiple copies of the same sample are tested simultaneously under different heating conditions.

6.1.5   RC parameter

Due to the inherent limitations of several figures of merit, which are related to the variable outdoor conditions under which they can be tested, Li *et al.* [40], proposed to use a simple metric called *RC*, which can be computed as follows:

$$RC = \varepsilon_{sky} - r(1 - R_{solar}),\qquad(4)$$

where ε_{sky} is the emissivity in the sky window, R_{solar} is a total reflectance in the solar spectrum, and r is the ratio of the solar irradiation power over the blackbody surface emissive power transmitted through the sky window. *RC* should be used to compare different PDRC materials at the same solar irradiation and weather conditions. The authors recommend using the "standard *RC*" by referring to a standard surface temperature of 300 K to calculate the emissivity, and using a standard r value of 10 (a typical peak solar irradiation of 1000 W m^{-2} and blackbody emissive power 100 W m^{-2}). The *RC* parameter has been used in various studies to compare different PDRC materials as it conveniently condenses the basic information about the emissivity and reflectance spectrum in one figure which does not depend on environmental conditions. However, the *RC* value cannot differentiate between broadband/narrow-band emitters, nor does it contemplate the angular dependence of the emissivity.

A different figure of merit was also proposed by Zhang *et al.* [88], called the cooling performance coefficient C_p:

$$C_p = 0.57 \cdot R_{solar} + 0.43 \cdot \varepsilon_{sky}.\qquad(5)$$

However, the weighing factors in the equations are determined from the results of previous experiments, which makes this figure of merit less universal than the one proposed by Li *et al*.

6.2   Cooling performance-based parameters

Rather than comparing the properties of the materials and basic parameters of the cooling process, some studies present broader indicators of the cooling efficiency in real applications. One of these indicators is the roof thermal transfer value (*RTTV*). This parameter is based on a model for calculating heat gain or loss through roofs depending on various parameters and it is a powerful tool for designing new types of roofs and controlling the energy usage in buildings. *RTTV* is given in W m^{-2} or, in a monthly cumulative form, in kWh m^{-2}. Fang *et al.* [89] improved the common *RTTV* model to be used with a novel PDRC material (RadiCold film [90]). *RTTV* values are then presented to prove that a roof coated by RadiCold performs better

in terms of temperature management and can be used for long-time passive cooling of non-residential buildings.

In various PDRC applications, results are presented in the form of energy balance of the space to be cooled. For example, annual cooling electricity consumption (in kWh) for buildings with and without PDRC elements can be compared [91], highlighting a positive effect of this approach. Alternatively, some studies use an analysis of cooling costs reduction based on the energy savings.

For proposing a fitting PDRC material for an application at a specific location, the cooling degree day (*CDD*) method can also be used. This figure predicts how much cooling is needed in buildings to reach a long-time temperature comfort. Even though this method is not necessarily linked to PDRC, it can help in designing new cooling elements for specific buildings [92].

6.3   Numerical methods for PDRC materials comparison

The lack of universal comparison methods for PDRC materials has been addressed by some researchers using numerical modelling methods.

Yu *et al.* gathered information on 55 different radiative cooling materials from 45 studies and compared their corresponding cooling power [30], as can be seen in Figure 27. They used available spectral data (absorptivity/emissivity) in the 0.3 – 20 µm range, standard AM 1.5 solar spectrum for solar irradiance and MODTRAN application for calculating spectral radiance at the US standard model atmosphere. In a previous work from the same group [66], all six model atmospheres from MODTRAN were considered, with the US standard model providing the best results (as previously seen in Figure 14). The full set of equations used for the calculation consists of expressions for all of the elements in Equation 3. P_{nonrad} was neglected in this study, therefore the authors point out that resulting cooling powers might be higher than experimental results. The obtained values are however still useful to compare the cooling ability of different materials under standardised conditions.
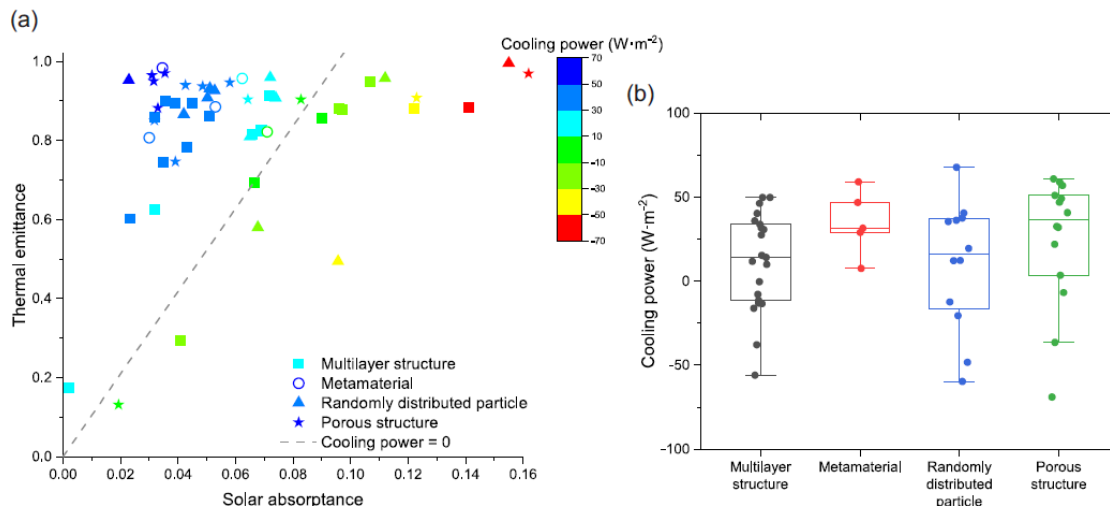
Figure 27: Colour-coded map of radiative cooling materials compared by Yu et al. (a) Calculated cooling power as a function of thermal emittance and solar absorbance, (b) comparison of different PDRC materials [30].

Calculating the assumed cooling power from the obtainable spectral data and simulated atmospheric condition seems to be a promising tool for comparison of the PDRC materials. Albeit on a smaller scale, a similar study was also conducted by Wray *et al.* [93]. Next to the commonly used MODTRAN application, the transmittance-based cosine model is also frequently used for approximating the infrared atmospheric radiance. Compared to MODTRAN, approximated transmittance-based models lead to >10% systematic cooling power underestimations. However, Mandal *et al.* presented a temperature correction [94] to the traditional model, suggesting that the corrected model represents an improvement as it retains the useful angular resolution, which the MODTRAN hemispherical irradiance model does not provide. In the PaRaMetriC project, a model

for the calculation of radiation heat exchanges with the atmosphere will be developed, based on a combination of the longwave Rapid Radiative Transfer Model (RRTM) [95] and the climatic parameters obtained from the European Centre for Medium-Range Weather Forecasts (ECMWF) ERA5 database [96].

6.4   Experimental methods for PDRC materials comparison

Next to the universal numerical methods, standardised experimental setups for PDRC materials comparison have also been taken into consideration in recent years. Yoon et al. comment on the fact that the already-used indicators of PDRC performance deal only with a small thermal mass of a sample, and do not consider the real-world systems to which the radiative cooler is applied. Therefore, they built an experimental apparatus for a direct measurement of the average daily cooling power as well as the resulting cooling energy reduction [97]. The apparatus (Figure 28) consists of two identical enclosures to be coated with two materials that one intends to compare, complemented with multiple thermoelectric coolers attached through the walls to enable the active control of the enclosure temperatures. The authors conducted two different outdoor experiments: one with constant enclosure temperature and the other with a constant temperature difference between the enclosure and ambient. This setup can provide direct comparison of two PDRC performances at similar experimental conditions, as well as an estimation of the cooling load reduction (when measuring enclosures with and without PDRC properties).
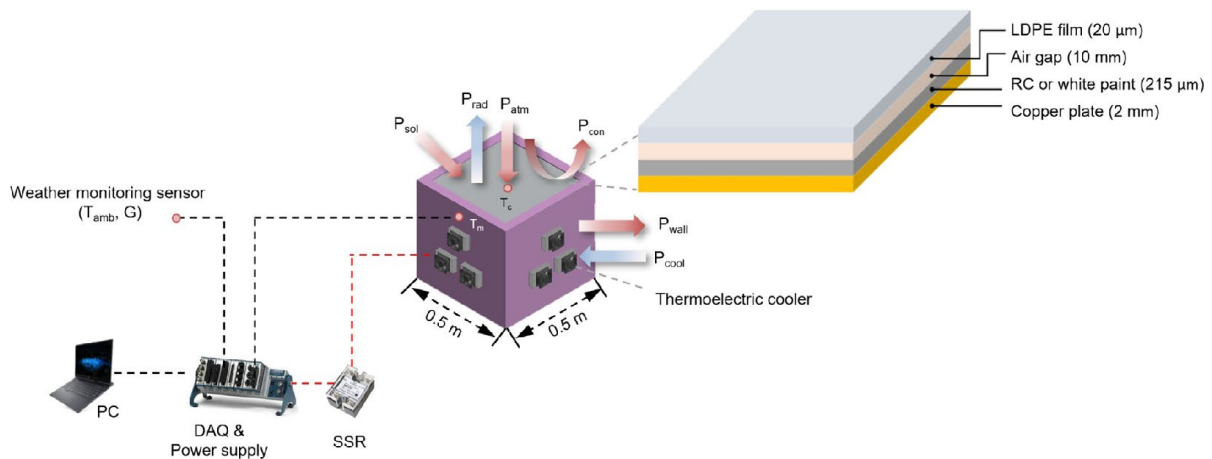
Figure 28: ½ of an experimental setup for a direct PDRC measurements comparison [97].

Fan *et al.* also used two devices, which however are meant to study two specimens of the same material [98]. The main idea of this approach is to be able to measure both maximum sub-ambient temperature reduction and a maximum net cooling power for the same material (Figure 29) under otherwise identical conditions. By measuring these properties simultaneously, this method is able to decouple the radiative and non-radiative heat transfer contributions. The authors suggest that for more precise comparison of various PDRC materials from literature, maximum sub-ambient temperature drop should be reported together with the non-radiative heat transfer coefficient.

Figure 29: Experimental setup for measurement of two identical PDRC samples [98].

Bu *et al.* states that reporting both maximum net cooling power and maximum sub-ambient temperature reduction with the external parameters of PDRC testing is crucial for direct material comparison. However, temperature variations among different studies can significantly affect the comparison, which creates a demand for standardised data reporting [77]. In their study, the authors suggest several points for PDRC testing:

1) Measurement should be conducted to cover noon hours (10 a.m. to 2 p.m.) to test the cooler under peak solar irradiation.

2) A direct photograph of the sky could provide an initial estimation of the cloud coverage.

3) Measured cooling power should be converted to the ambient temperature value of 25 °C. Converting can be performed by the scaling [41] of P_{rad} and P_{atm} (Equation 3)
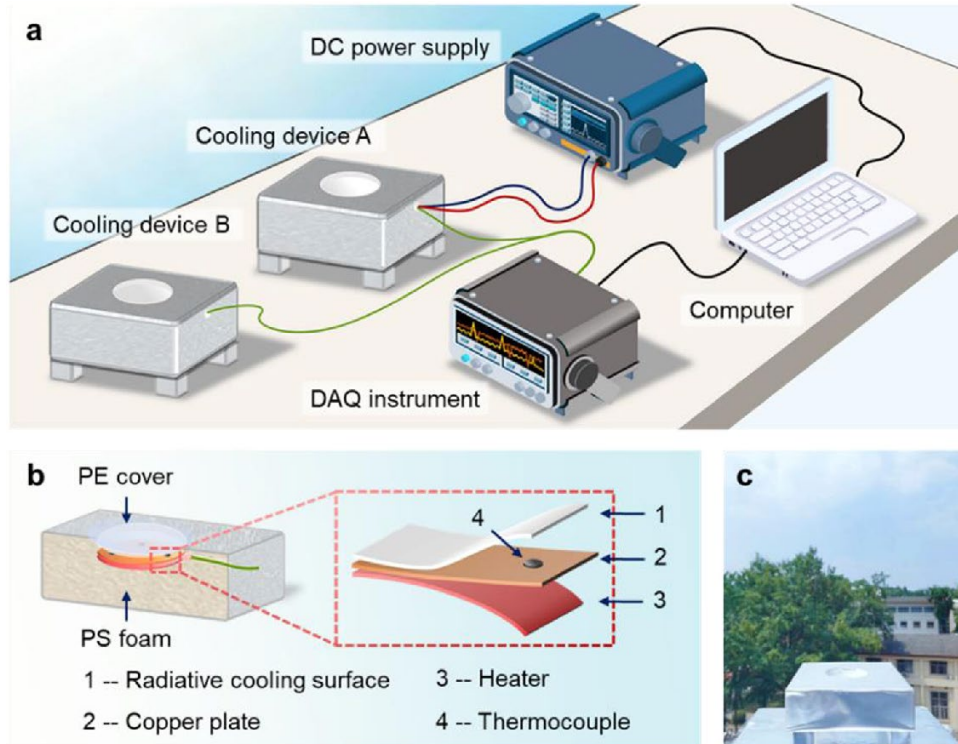
4) Ambient temperature measurements should be performed inside a Stevenson screen placed around 1.5 m above ground to prevent ground solar reflection and heat conduction. Temperature of the PDRC material should be measured at multiple points.

5) Wind cover should be used to minimise the influence of the non-radiative heat transfer. Strong ambient wind significantly exacerbates the cooling power uncertainty by introducing intense and rapidly varying fluctuations. It is desirable for the cooling setup to contain top, side and bottom insulation.

Possible standardisation of outdoor PDRC tests was discussed also by Zhou *et al.* [99]. According to this comment, reporting the observed PDRC performance only during selected days with favourable weather conditions is problematic, long-term data should be reported instead. Using average cooling ability in seasonal climate conditions gives a better view of the obtained cooling potential. Comparison with a seasonal performance of conventional air-conditioning utility is also desirable. The authors of the comment recommend EnergyPlus modelling to simultaneously estimate possible energy savings of new cooling materials.

In order to improve reproducibility of the measurement, indoor test standardisation has also been proposed. Song *et al.* designed indoor equipment as a tool for universal PDRC performance comparison [100]. Using an

Aluminium dome cooled down by liquid nitrogen and complemented with a solar simulator, outdoor night-time and daytime conditions can be simulated in a laboratory environment. Similar setup can be found in the work of Park *et al.* [101], who reduced the radiation from the participating media by filling the chamber with nitrogen gas and also ensured a view factor of 0.99 for the emitter. Even though the outdoor condition cannot be fully reproduced, and especially the complex role of the whole atmospheric column, this approach to PDRC testing standardisation indicates a possible strategy to improve the comparability among different PDRC materials.

7 Conclusions and recommendations

This report on the current studies published on the topic of PDRC showed that the identification of universal figures of merit for PDRC materials remains as one of the major challenges in the field. Most of the studies suggest considering two basic indicators: maximum sub-ambient temperature drop and cooling power at ambient temperature, but a whole set of experimental conditions is needed to fully describe the PDRC performance of a given material. Some numerical methods have been suggested to approximately compare cooling materials using standard model atmospheres and other simplifications. However, for a more precise and effective comparison, the implementation of standard indoor or outdoor experimental test methods is needed in the scientific community.

Given the large number of application fields where PDRC materials can be applied (see Section 4.2), and the increasing number of companies which are currently developing products based on this technology, it is clear that the development of standardisation methods to certify their performance become essential to ensure the quality and reliability of these products and promote their market adoption.

Based on the findings reported in this document, in the following we indicate a recommended list of parameters that should be ideally reported from experimental PDRC measurement.

Material properties:

- solar reflectivity at least in the wavelength range between 0.3 µm and 2.5 µm

- angular and spectrally resolved emissivity between 2.5 and 25 µm

- thermal resistivity across the PDRC material

PDRC performance:

- maximum temperature drop and cooling power at ambient temperature measured simultaneously for two identical samples of the material under test, during both daytime and night-time hours (night-time measurements can be used to isolate the contribution of the infrared emissivity)

- same as above, for two additional identical samples of a suitable PDRC material with well-known properties

Experimental conditions:

- time, date and location of the experiment, to allow subsequent modelling of the relevant atmospheric conditions and composition

- relative tilting angle between the emitter and the sky

- if the PDRC performance measurements are performed in an enclosed measurement box, ambient temperature and humidity should be reported both inside and outside the box, using properly shielded temperature sensors

- total solar irradiance

- downwelling long-wave radiation and/or IR camera pictures of the sky conditions during the experiment

- wind speed (especially in the case of experiments performed without convection shield)

This list should not be considered exhaustive or suitable to all potential applications of PDRC materials. As discussed in the previous sections, specific applications may require additional figures of merit, or even a different set of custom performance indicators. Some notable examples include for instance cooling textiles, which should of course be also flexible, breathable and capable of undergoing several washing cycles. In the agricultural, packing and food sectors, properties such as recyclability, non-toxicity or even biodegradability of the employed PDRC materials (e.g., using biopolymers such as cellulose or chitosan) may in certain cases

become particularly desirable, in contrast with typical durability requirements of other applications. In other scenarios, instead, the above mentioned figures of merit may still be applicable, but with rather different boundary conditions. Two opposite examples are given by the passive cooling of electric vehicles shells (which will need to work under extremely different convective losses with respect to static objects) or spacecraft, where non-radiative losses are basically absent, but PDRC materials are exposed to much harsher conditions of strong particle and electromagnetic irradiation, extreme thermal cycles, as well as exposure to highly reactive atomic oxygen.

Finally, even in the building sector, several other figures of merit may be equally relevant than the few ones mentioned here. Aesthetic, safety and added weight should also be considered carefully. One limitation of PDRC materials is that their visual appearance is basically limited to either specularly reflective, or diffuse white. Highly specular reflective surfaces may cause glaring reflections which may disturb or pose safety issues, compared to a white diffuse finish. Safety regulations may pose additional constraints, e.g., in terms of fire resistance or at least fire retardancy properties that many PDRC materials may not currently fulfil. And finally, highly effective paint-like PDRC materials require very high mass fractions of pigments and large layer thickness around 0.5 mm, which would easily result in >1 kg m^{-2} of added weight, which should be duly considered by engineers, especially for roof applications.

8 References

1. Chen, M.; Pang, D.; Chen, X.; Yan, H.; Yang, Y., Passive daytime radiative cooling: Fundamentals, material designs, and applications. *EcoMat* **2022,** *4* (1), e12153. https://doi.org/10.1002/eom2.12153

2. Zhao, B.; Hu, M.; Ao, X.; Pei, G., Performance evaluation of daytime radiative cooling under different clear sky conditions. *Applied Thermal Engineering* **2019,** *155*, 660-666. https://doi.org/10.1016/j.applthermaleng.2019.04.028

3. Barker, R., The Process of Making Ice in the East Indies. By Sir Robert Barker, F. R. S. in a Letter to Dr. Brocklesby. *Philosophical Transactions (1683-1775)* **1775,** *65*, 252-257. https://doi.org/10.1098/rstl.1775.0023

4. Catalanotti, S.; Cuomo, V.; Piro, G.; Ruggi, D.; Silvestrini, V.; Troise, G., The radiative cooling of selective surfaces. *Solar Energy* **1975,** *17* (2), 83-89. https://doi.org/10.1016/0038-092X(75)90062-6

5. Raman, A. P.; Anoma, M. A.; Zhu, L.; Rephaeli, E.; Fan, S., Passive radiative cooling below ambient air temperature under direct sunlight. *Nature* **2014,** *515* (7528), 540-544. http://dx.doi.org/10.1038/nature13883

6. Fernandez, N.; Wang, W.; Alvine, K. J.; Katipamula, S. In *Energy Savings Potential of Radiative Cooling Technologies*, 2015.

7. Peoples, J.; Hung, Y.-W.; Li, X.; Gallagher, D.; Fruehe, N.; Pottschmidt, M.; Breseman, C.; Adams, C.; Yuksel, A.; Braun, J.; Horton, W. T.; Ruan, X., Concentrated radiative cooling. *Applied Energy* **2022,** *310*, 118368. https://doi.org/10.1016/j.apenergy.2021.118368

8. Mandal, J.; Yang, Y.; Yu, N.; Raman, A. P., Paints as a Scalable and Effective Radiative Cooling Technology for Buildings. *Joule* **2020,** *4* (7), 1350-1356. https://doi.org/10.1016/j.joule.2020.04.010

9. Chen, J.; Lu, L., Comprehensive evaluation of thermal and energy performance of radiative roof cooling in buildings. *Journal of Building Engineering* **2021,** *33*, 101631. https://doi.org/10.1016/j.jobe.2020.101631

10. Fortin, R.; Mandal, J.; Raman, A. P.; Craig, S., Passive radiative cooling to sub-ambient temperatures inside naturally ventilated buildings. *Cell Reports Physical Science* **2023,** *4* (9), 101570. https://doi.org/10.1016/j.xcrp.2023.101570

11. Zhao, D.; Aili, A.; Yin, X.; Tan, G.; Yang, R., Roof-integrated radiative air-cooling system to achieve cooler attic for building energy saving. *Energy and Buildings* **2019,** *203*, 109453. https://doi.org/10.1016/j.enbuild.2019.109453

12. Goldstein, E. A.; Raman, A. P.; Fan, S., Sub-ambient non-evaporative fluid cooling with the sky. *Nature Energy* **2017,** *2* (9), 17143. http://dx.doi.org/10.1038/nenergy.2017.143

13. Aili, A.; Zhao, D.; Lu, J.; Zhai, Y.; Yin, X.; Tan, G.; Yang, R., A kW-scale, 24-hour continuously operational, radiative sky cooling system: Experimental demonstration and predictive modeling. *Energy Conversion and Management* **2019,** *186*, 586-596. https://doi.org/10.1016/j.enconman.2019.03.006

14. Mokhtari, R.; Ulpiani, G.; Ghasempour, R., The Cooling Station: Combining hydronic radiant cooling and daytime radiative cooling for urban shelters. *Applied Thermal Engineering* **2022,** *211*, 118493. https://doi.org/10.1016/j.applthermaleng.2022.118493

15. Vilà, R.; Medrano, M.; Castell, A., Numerical analysis of the combination of radiative collectors and emitters to improve the performance of water-water compression heat pumps under different climates. *Energy* **2023,** *266*, 126445. https://doi.org/10.1016/j.energy.2022.126445

16. Bijarniya, J.; Sarkar, J.; Maiti, P., Review on passive daytime radiative cooling: Fundamentals, recent researches, challenges and opportunities. *Renewable and Sustainable Energy Reviews* **2020,** *133*, 110263. https://doi.org/10.1016/j.rser.2020.110263

17. Pakdel, E.; Wang, X., Thermoregulating textiles and fibrous materials for passive radiative cooling functionality. *Materials & Design* **2023,** *231*, 112006. https://doi.org/10.1016/j.matdes.2023.112006

18. Zhou, Z.; Wang, Z.; Bermel, P., Radiative cooling for low-bandgap photovoltaics under concentrated sunlight. *Opt. Express* **2019,** *27* (8), A404-A418. https://doi.org/10.1364/OE.27.00A404

19. Zhou, M.; Song, H.; Xu, X.; Shahsafi, A.; Qu, Y.; Xia, Z.; Ma, Z.; Kats, M. A.; Zhu, J.; Ooi, B. S.; Gan, Q.; Yu, Z., Vapor condensation with daytime radiative cooling. *Proceedings of the National Academy of Sciences* **2021,** *118* (14), e2019292118. https://doi.org/10.1073/pnas.2019292118

20. Li, J.; Liang, Y.; Li, W.; Xu, N.; Zhu, B.; Wu, Z.; Wang, X.; Fan, S.; Wang, M.; Zhu, J., Protecting ice from melting under sunlight via radiative cooling. *Science Advances* **2022,** *8* (6), eabj9756. https://doi.org/10.1126/sciadv.abj9756

21.   Elgendi, M.; Tamimi, J. A. L.; Alfalahi, A.; Alkhoori, D.; Alshanqiti, M.; Aladawi, A., Wall panels using thermoelectric generators for sustainable cities and communities: a mini-review. *IOP Conference Series: Earth and Environmental Science* **2022,** *1074* (1), 012003. https://doi.org/10.1088/1755-1315/1074/1/012003

22.   Huang, X.; Mandal, J.; Xu, J.; Raman, A. P., Passive freezing desalination driven by radiative cooling. *Joule* **2022,** *6* (12), 2762-2775. https://doi.org/10.1016/j.joule.2022.10.009

23.   Li, W.; Shi, Y.; Chen, K.; Zhu, L.; Fan, S., A Comprehensive Photonic Approach for Solar Cell Cooling. *ACS Photonics* **2017,** *4* (4), 774-782. https://doi.org/10.1021/acsphotonics.7b00089

24.   Zou, H.; Wang, C.; Yu, J.; Huang, D.; Yang, R.; Wang, R., Eliminating greenhouse heat stress with transparent radiative cooling film. *Cell Reports Physical Science* **2023,** *4* (8), 101539. https://doi.org/10.1016/j.xcrp.2023.101539

25.   Xiao, W.; Dai, P.; Singh, H. J.; Ajia, I. A.; Yan, X.; Wiecha, P. R.; Huang, R.; de Groot, C. H.; Muskens, O. L.; Sun, K., Flexible thin film optical solar reflectors with Ta2O5-based multimaterial coatings for space radiative cooling. *APL Photonics* **2023,** *8* (9), 090802. https://doi.org/10.1063/5.0156526

26.   Aili, A.; Wei, Z. Y.; Chen, Y. Z.; Zhao, D. L.; Yang, R. G.; Yin, X. B., Selection of polymers with functional groups for daytime radiative cooling. *Materials Today Physics* **2019,** *10*, 100127. https://doi.org/10.1016/j.mtphys.2019.100127

27.   Tong, Z.; Peoples, J.; Li, X.; Yang, X.; Bao, H.; Ruan, X., Electronic and phononic origins of BaSO4 as an ultra-efficient radiative cooling paint pigment. *Materials Today Physics* **2022,** *24*, 100658. https://doi.org/10.1016/j.mtphys.2022.100658

28.   Zhao, B.; Hu, M.; Ao, X.; Chen, N.; Pei, G., Radiative cooling: A review of fundamentals, materials, applications, and prospects. *Applied Energy* **2019,** *236*, 489-513. https://doi.org/10.1016/j.apenergy.2018.12.018

29.   Kousis, I.; Pisello, A. L., Toward the Scaling up of Daytime Radiative Coolers: A Review. *Advanced Optical Materials* **2023,** *n/a* (n/a), 2300123. https://doi.org/10.1002/adom.202300123

30.   Yu, X.; Chan, J.; Chen, C., Review of radiative cooling materials: Performance evaluation and design approaches. *Nano Energy* **2021,** *88*, 106259. https://doi.org/10.1016/j.nanoen.2021.106259

31.   Zhang, J.; Yuan, J.; Liu, J.; Zhou, Z.; Sui, J.; Xing, J.; Zuo, J., Cover shields for sub-ambient radiative cooling: A literature review. *Renewable and Sustainable Energy Reviews* **2021,** *143*, 110959. https://doi.org/10.1016/j.rser.2021.110959

32.   Yang, M.; Zou, W.; Guo, J.; Qian, Z.; Luo, H.; Yang, S.; Zhao, N.; Pattelli, L.; Xu, J.; Wiersma, D. S., Bioinspired "Skin" with Cooperative Thermo-Optical Effect for Daytime Radiative Cooling. *ACS Applied Materials & Interfaces* **2020,** *12* (22), 25286-25293. https://doi.org/10.1021/acsami.0c03897

33.   Liu, J.; Tang, H.; Zhang, J.; Zhang, D.; Jiao, S.; Zhou, Z., Boosting daytime radiative cooling performance with nanoporous polyethylene film. *Energy and Built Environment* **2023,** *4* (2), 131-139. https://doi.org/10.1016/j.enbenv.2021.10.001

34.   Leroy, A.; Bhatia, B.; Kelsall, C. C.; Castillejo-Cuberos, A.; Di Capua H., M.; Zhao, L.; Zhang, L.; Guzman, A. M.; Wang, E. N., High-performance subambient radiative cooling enabled by optically selective and thermally insulating polyethylene aerogel. *Science Advances* **2019,** *5* (10), eaat9480. https://doi.org/10.1126/sciadv.aat9480

35.   Torgerson, E.; Hellhake, J., Polymer solar filter for enabling direct daytime radiative cooling. *Solar Energy Materials and Solar Cells* **2020,** *206*, 110319. https://doi.org/10.1016/j.solmat.2019.110319

36.   Miao, D.; Wang, X.; Yu, J.; Ding, B., Nanoengineered Textiles for Outdoor Personal Cooling and Drying. *Advanced Functional Materials* **2022,** *32* (51), 2209029. https://doi.org/10.1002/adfm.202209029

37.   Li, T.; Zhai, Y.; He, S.; Gan, W.; Wei, Z.; Heidarinejad, M.; Dalgo, D.; Mi, R.; Zhao, X.; Song, J.; Dai, J.; Chen, C.; Aili, A.; Vellore, A.; Martini, A.; Yang, R.; Srebric, J.; Yin, X.; Hu, L., A radiative cooling structural material. *Science* **2019,** *364* (6442), 760-763. https://doi.org/10.1126/science.aau9101

38.   Li, T.; Sun, H.; Yang, M.; Zhang, C.; Lv, S.; Li, B.; Chen, L.; Sun, D., All-Ceramic, compressible and scalable nanofibrous aerogels for subambient daytime radiative cooling. *Chemical Engineering Journal* **2023,** *452*, 139518. https://doi.org/10.1016/j.cej.2022.139518

39.   Chan, K.-Y.; Shen, X.; Yang, J.; Lin, K.-T.; Venkatesan, H.; Kim, E.; Zhang, H.; Lee, J.-H.; Yu, J.; Yang, J.; Kim, J.-K., Scalable anisotropic cooling aerogels by additive freeze-casting. *Nature Communications* **2022,** *13* (1), 5553. https://doi.org/10.1038/s41467-022-33234-8

40.   Li, X.; Peoples, J.; Huang, Z.; Zhao, Z.; Qiu, J.; Ruan, X., Full Daytime Sub-ambient Radiative Cooling in Commercial-like Paints with High Figure of Merit. *Cell Reports Physical Science* **2020,** *1* (10), 100221. https://doi.org/10.1016/j.xcrp.2020.100221

41. Li, X.; Peoples, J.; Yao, P.; Ruan, X., Ultrawhite BaSO4 Paints and Films for Remarkable Daytime Subambient Radiative Cooling. *ACS Applied Materials & Interfaces* **2021,** *13* (18), 21733-21739. https://doi.org/10.1021/acsami.1c02368

42. Mandal, J.; Fu, Y.; Overvig, A. C.; Jia, M.; Sun, K.; Shi, N. N.; Zhou, H.; Xiao, X.; Yu, N.; Yang, Y., Hierarchically porous polymer coatings for highly efficient passive daytime radiative cooling. *Science* **2018,** *362* (6412), 315-319. https://doi.org/10.1126/science.aat9513

43. Sonne, C.; Jenssen, B. M.; Rinklebe, J.; Lam, S. S.; Hansen, M.; Bossi, R.; Gustavson, K.; Dietz, R., EU need to protect its environment from toxic per- and polyfluoroalkyl substances. *Science of The Total Environment* **2023,** *876*, 162770. https://doi.org/10.1016/j.scitotenv.2023.162770

44. Tyrrell, N. D., A Proposal That Would Ban Manufacture, Supply, and Use of All Fluoropolymers and Most Fluorinated Reagents within the Entire EU. *Organic Process Research & Development* **2023,** *27* (8), 1422-1426. https://doi.org/10.1021/acs.oprd.3c00199

45. Zhou, L.; Song, H.; Liang, J.; Singer, M.; Zhou, M.; Stegenburgs, E.; Zhang, N.; Xu, C.; Ng, T.; Yu, Z.; Ooi, B.; Gan, Q., A polydimethylsiloxane-coated metal structure for all-day radiative cooling. *Nature Sustainability* **2019,** *2* (8), 718-724. https://doi.org/10.1038/s41893-019-0348-5

46. Banik, U.; Agrawal, A.; Meddeb, H.; Sergeev, O.; Reininghaus, N.; Götz-Köhler, M.; Gehrke, K.; Stührenberg, J.; Vehse, M.; Sznajder, M.; Agert, C., Efficient Thin Polymer Coating as a Selective Thermal Emitter for Passive Daytime Radiative Cooling. *ACS Applied Materials & Interfaces* **2021,** *13* (20), 24130-24137. https://doi.org/10.1021/acsami.1c04056

47. Huang, X.; Mandal, J.; Raman, A., Do-it-yourself radiative cooler as a radiative cooling standard and cooling component for device design. *Journal of Photonics for Energy* **2021,** *12* (1), 012112. https://doi.org/10.1117/1.JPE.12.012112

48. Castaldo, A.; Vitiello, G.; Gambale, E.; Lanchi, M.; Ferrara, M.; Zinzi, M., Mirroring Solar Radiation Emitting Heat Toward the Universe: Design, Production, and Preliminary Testing of a Metamaterial Based Daytime Passive Radiative Cooler. *Energies* **2020,** *13* (16), 4192. https://doi.org/10.3390/en13164192

49. Chae, D.; Kim, M.; Jung, P.-H.; Son, S.; Seo, J.; Liu, Y.; Lee, B. J.; Lee, H., Spectrally Selective Inorganic-Based Multilayer Emitter for Daytime Radiative Cooling. *ACS Applied Materials & Interfaces* **2020,** *12* (7), 8073-8081. https://doi.org/10.1021/acsami.9b16742

50. Feng, J.; Gao, K.; Santamouris, M.; Shah, K. W.; Ranzi, G., Dynamic impact of climate on the performance of daytime radiative cooling materials. *Solar Energy Materials and Solar Cells* **2020,** *208*, 110426. https://doi.org/10.1016/j.solmat.2020.110426

51. Liu, C.; Wu, Y.; Wang, B.; Zhao, C. Y.; Bao, H., Effect of atmospheric water vapor on radiative cooling performance of different surfaces. *Solar Energy* **2019,** *183*, 218-225. https://doi.org/10.1016/j.solener.2019.03.011

52. Tso, C. Y.; Chan, K. C.; Chao, C. Y. H., A field investigation of passive radiative cooling under Hong Kong's climate. *Renewable Energy* **2017,** *106*, 52-61. https://doi.org/10.1016/j.renene.2017.01.018

53. Yang, Y.; Zhang, G.; Rong, L., Impact of cloud and total column water vapor on annual performance of passive daytime radiative cooler. *Energy Conversion and Management* **2022,** *273*, 116420. https://doi.org/10.1016/j.enconman.2022.116420

54. Aili, A.; Yin, X.; Yang, R., Passive sub-ambient cooling: radiative cooling versus evaporative cooling. *Applied Thermal Engineering* **2022,** *202*, 117909. https://doi.org/10.1016/j.applthermaleng.2021.117909

55. Huang, J.; Lin, C.; Li, Y.; Huang, B., Effects of humidity, aerosol, and cloud on subambient radiative cooling. *International Journal of Heat and Mass Transfer* **2022,** *186*, 122438. https://doi.org/10.1016/j.ijheatmasstransfer.2021.122438

56. Wang, T.; Wu, Y.; Shi, L.; Hu, X.; Chen, M.; Wu, L., A structural polymer for highly efficient all-day passive radiative cooling. *Nature Communications* **2021,** *12* (1), 365. https://doi.org/10.1038/s41467-020-20646-7

57. Lin, K.-T.; Han, J.; Li, K.; Guo, C.; Lin, H.; Jia, B., Radiative cooling: Fundamental physics, atmospheric influences, materials and structural engineering, applications and beyond. *Nano Energy* **2021,** *80*, 105517. https://doi.org/10.1016/j.nanoen.2020.105517

58. Simsek, E.; Mandal, J.; Raman, A. P.; Pilon, L., Dropwise condensation reduces selectivity of sky-facing radiative cooling surfaces. *International Journal of Heat and Mass Transfer* **2022,** *198*, 123399. https://doi.org/10.1016/j.ijheatmasstransfer.2022.123399

59. Tao, S.; Xu, X.; Chen, M.; Xu, W.; Li, L.; Fang, Z.; Zhu, C.; Lu, C.; Xu, Z., Construction of efficient passive radiative cooling emitter with selective emission in the whole atmospheric window and durable anti-

contamination performance. *Solar Energy Materials and Solar Cells* **2021,** *224*, 110998. https://doi.org/10.1016/j.solmat.2021.110998

60.   Mokhtari, R.; Fakouriyan, S.; Ghasempour, R., Investigating the Effect of Cloud Cover on Radiative Cooling Potential With Artificial Neural Network Modeling. *Frontiers in Energy Research* **2021,** *9*. https://doi.org/10.3389/fenrg.2021.658338

61.   Chen, Z.; Zhu, L.; Raman, A.; Fan, S., Radiative cooling to deep sub-freezing temperatures through a 24-h day–night cycle. *Nature Communications* **2016,** *7* (1), 13729. http://dx.doi.org/10.1038/ncomms13729

62.   Leroy, A.; Bhatia, B.; Sircar, J.; Wang, E. N., Thermal transport in solar-reflecting and infrared-transparent polyethylene aerogels. *International Journal of Heat and Mass Transfer* **2022,** *184*, 122307. https://doi.org/10.1016/j.ijheatmasstransfer.2021.122307

63.   Qin, J.; Zhang, Z.; Li, Y.; Cai, Y.; Zhang, H.; Liu, L.; Xu, L.; Zhang, W.; Xue, X., Design and manufacture of a radiative cooler to measure the subambient cooling effect and cooling power. *Review of Scientific Instruments* **2022,** *93* (5), 054901. https://doi.org/10.1063/5.0087494

64.   Liu, J.; Zhang, J.; Zhang, D.; Jiao, S.; Xing, J.; Tang, H.; Zhang, Y.; Li, S.; Zhou, Z.; Zuo, J., Sub-ambient radiative cooling with wind cover. *Renewable and Sustainable Energy Reviews* **2020,** *130*, 109935. https://doi.org/10.1016/j.rser.2020.109935

65.   Liu, J.; Zhou, Z.; Zhang, D.; Jiao, S.; Zhang, Y.; Luo, L.; Zhang, Z.; Gao, F., Field investigation and performance evaluation of sub-ambient radiative cooling in low latitude seaside. *Renewable Energy* **2020,** *155*, 90-99. https://doi.org/10.1016/j.renene.2020.03.136

66.   Yu, X.; Chen, C., A simulation study for comparing the cooling performance of different daytime radiative cooling materials. *Solar Energy Materials and Solar Cells* **2020,** *209*, 110459. https://doi.org/10.1016/j.solmat.2020.110459

67.   Vilà, R.; Medrano, M.; Castell, A., Mapping Nighttime and All-Day Radiative Cooling Potential in Europe and the Influence of Solar Reflectivity. *Atmosphere* **2021,** *12* (9), 1119. https://doi.org/10.3390/atmos12091119

68.   Vilà, R.; Medrano, M.; Castell, A., Climate change influences in the determination of the maximum power potential of radiative cooling. Evolution and seasonal study in Europe. *Renewable Energy* **2023,** *212*, 500-513. https://doi.org/10.1016/j.renene.2023.05.083

69.   Herrmann, K.; Lauster, T.; Song, Q.; Retsch, M., Homogeneous Polymer Films for Passive Daytime Cooling: Optimized Thickness for Maximized Cooling Performance. *Advanced Energy and Sustainability Research* **2022,** *3*. https://doi.org/10.1002/aesr.202100166

70.   Zhao, Y.; Pang, D.; Chen, M.; Chen, Z.; Yan, H., Scalable aqueous processing-based radiative cooling coatings for heat dissipation applications. *Applied Materials Today* **2022,** *26*, 101298. https://doi.org/10.1016/j.apmt.2021.101298

71.   Felicelli, A.; Katsamba, I.; Barrios, F.; Zhang, Y.; Guo, Z.; Peoples, J.; Chiu, G.; Ruan, X., Thin layer lightweight and ultrawhite hexagonal boron nitride nanoporous paints for daytime radiative cooling. *Cell Reports Physical Science* **2022,** *3* (10), 101058. https://doi.org/10.1016/j.xcrp.2022.101058

72.   Jeon, S.; Shin, J., Directional radiation for optimal radiative cooling. *Opt. Express* **2021,** *29* (6), 8376-8386. https://doi.org/10.1364/OE.416475

73.   Liu, J.; Zhang, D.; Jiao, S.; Zhou, Z.; Zhang, Z.; Gao, F., Daytime radiative cooling with clear epoxy resin. *Solar Energy Materials and Solar Cells* **2020,** *207*, 110368. https://doi.org/10.1016/j.solmat.2019.110368

74.   Zhao, B.; Ao, X.; Chen, N.; Xuan, Q.; Hu, M.; Pei, G., General strategy of passive sub-ambient daytime radiative cooling. *Solar Energy Materials and Solar Cells* **2019,** *199*, 108-113. https://doi.org/10.1016/j.solmat.2019.04.028

75.   Zhou, L.; Song, H.; Zhang, N.; Rada, J.; Singer, M.; Zhang, H.; Ooi, B. S.; Yu, Z.; Gan, Q., Hybrid concentrated radiative cooling and solar heating in a single system. *Cell Reports Physical Science* **2021,** *2* (2), 100338. https://doi.org/10.1016/j.xcrp.2021.100338

76.   Dong, M.; Zhu, L.; Jiang, B.; Fan, S.; Chen, Z., Concentrated radiative cooling and its constraint from reciprocity. *Opt. Express* **2022,** *30* (1), 275-285. https://doi.org/10.1364/OE.445544

77.   Bu, K.; Huang, X.; Li, X.; Bao, H., Consistent Assessment of the Cooling Performance of Radiative Cooling Materials. *Advanced Functional Materials* **2023,** *n/a* (n/a), 2307191. https://doi.org/10.1002/adfm.202307191

78.   Xu, C.; Ao, X.; Zhao, B.; Pei, G., A novel selective emissivity spectrum for radiative sky cooling. *Solar Energy Materials and Solar Cells* **2021,** *232*, 111380. https://doi.org/10.1016/j.solmat.2021.111380

79. Li, Y.; Li, L.; Guo, L.; An, B., Systematical analysis of ideal absorptivity for passive radiative cooling. *Opt. Mater. Express* **2020,** *10* (8), 1767-1777. https://doi.org/10.1364/OME.397617

80. Zeyghami, M.; Goswami, D. Y.; Stefanakos, E., A review of clear sky radiative cooling developments and applications in renewable power systems and passive building cooling. *Solar Energy Materials and Solar Cells* **2018,** *178*, 115-128. https://doi.org/10.1016/j.solmat.2018.01.015

81. Jeon, S.; Shin, J., Ideal spectral emissivity for radiative cooling of earthbound objects. *Scientific Reports* **2020,** *10* (1), 13038. https://doi.org/10.1038/s41598-020-70105-y

82. Kecebas, M. A.; Menguc, P.; Sendur, K., Spectral Emissivity Profiles for Radiative Cooling. *ACS Applied Optical Materials* **2023**. https://doi.org/10.1021/acsaom.3c00092

83. Chowdhary, A. K.; Bhowmik, T.; Sikdar, D., Infrared-blocking plasmonic meta-glass for energy-saving passive windows. *Opt. Lett.* **2022,** *47* (9), 2242-2245. https://doi.org/10.1364/OL.456134

84. Rephaeli, E.; Raman, A.; Fan, S., Ultrabroadband Photonic Structures To Achieve High-Performance Daytime Radiative Cooling. *Nano Letters* **2013,** *13* (4), 1457-1461. https://doi.org/10.1021/nl4004283

85. Ao, X.; Hu, M.; Zhao, B.; Chen, N.; Pei, G.; Zou, C., Preliminary experimental study of a specular and a diffuse surface for daytime radiative cooling. *Solar Energy Materials and Solar Cells* **2019,** *191*, 290-296. https://doi.org/10.1016/j.solmat.2018.11.032

86. Kong, A.; Cai, B.; Shi, P.; Yuan, X.-c., Ultra-broadband all-dielectric metamaterial thermal emitter for passive radiative cooling. *Opt. Express* **2019,** *27* (21), 30102-30115. https://doi.org/10.1364/OE.27.030102

87. Stanford Research Institute. Recommendations for Universal Testing of Radiative Cooling Technologies. Private communication.

88. Zhang, X.; Yang, L.; Wang, F.; Cheng, Z.; Liang, H., Wrinkled surface microstructure for enhancing the infrared spectral performance of radiative cooling. *Opt. Express* **2021,** *29* (8), 11416-11432. https://doi.org/10.1364/OE.418650

89. Fang, H.; Zhao, D.; Yuan, J.; Aili, A.; Yin, X.; Yang, R.; Tan, G., Performance evaluation of a metamaterial-based new cool roof using improved Roof Thermal Transfer Value model. *Applied Energy* **2019,** *248*, 589-599. https://doi.org/10.1016/j.apenergy.2019.04.116

90. Zhai, Y.; Ma, Y.; David, S. N.; Zhao, D.; Lou, R.; Tan, G.; Yang, R.; Yin, X., Scalable-manufactured randomized glass-polymer hybrid metamaterial for daytime radiative cooling. *Science* **2017,** *355* (6329), 1062-1066. https://doi.org/10.1126/science.aai7899

91. Jiang, K.; Zhang, K.; Shi, Z.; Li, H. In *Study on the cooling energy saving potential of a novel radiative cooling paints in building application*, E3S Web of Conferences, September 01, 2022; 2022; p 01074.

92. Hassan, S. A., The Role of Cooling Degree Days on determining the insulation of building Envelop in a hot climate (Iraqi cities as an example). *IOP Conference Series: Materials Science and Engineering* **2019,** *584* (1), 012009. http://dx.doi.org/10.1088/1757-899X/584/1/012009

93. Wray, P. R.; Su, M. P.; Atwater, H. A., Design of efficient radiative emission and daytime cooling structures with Si3N4 and SiO2 nanoparticle laminate films. *Opt. Express* **2020,** *28*, 35784. https://doi.org/10.1364/OE.408845

94. Mandal, J.; Huang, X.; Raman, A. P. Accurately Quantifying Clear-Sky Radiative Cooling Potentials: A Temperature Correction to the Transmittance-Based Approximation *Atmosphere* [Online], 2021. https://doi.org/10.3390/atmos12091195.

95. Mlawer, E. J.; Taubman, S. J.; Brown, P. D.; Iacono, M. J.; Clough, S. A., Radiative transfer for inhomogeneous atmospheres: RRTM, a validated correlated-k model for the longwave. *Journal of Geophysical Research: Atmospheres* **1997,** *102* (D14), 16663-16682. https://doi.org/10.1029/97JD00237

96. Hersbach, H.; Bell, B.; Berrisford, P.; Hirahara, S.; Horányi, A.; Muñoz-Sabater, J.; Nicolas, J.; Peubey, C.; Radu, R.; Schepers, D.; Simmons, A.; Soci, C.; Abdalla, S.; Abellan, X.; Balsamo, G.; Bechtold, P.; Biavati, G.; Bidlot, J.; Bonavita, M.; De Chiara, G.; Dahlgren, P.; Dee, D.; Diamantakis, M.; Dragani, R.; Flemming, J.; Forbes, R.; Fuentes, M.; Geer, A.; Haimberger, L.; Healy, S.; Hogan, R. J.; Hólm, E.; Janisková, M.; Keeley, S.; Laloyaux, P.; Lopez, P.; Lupu, C.; Radnoti, G.; de Rosnay, P.; Rozum, I.; Vamborg, F.; Villaume, S.; Thépaut, J.-N., The ERA5 global reanalysis. *Quarterly Journal of the Royal Meteorological Society* **2020,** *146* (730), 1999-2049. https://doi.org/10.1002/qj.3803

97. Yoon, S.; Chae, D.; Seo, J.; Choi, M.; Lim, H.; Lee, H.; Lee, B. J., Development of a device for characterizing radiative cooling performance. *Applied Thermal Engineering* **2022,** *213*, 118744. https://doi.org/10.1016/j.applthermaleng.2022.118744

98.   Fan, F.; Xu, D.; Zhu, Y.; Tan, G.; Zhao, D., A simple, accurate, and universal method for characterizing and comparing radiative cooling materials and devices. *International Journal of Heat and Mass Transfer* **2023,** *200*, 123494. https://doi.org/10.1016/j.ijheatmasstransfer.2022.123494

99.   Zhou, L.; Yin, X.; Gan, Q., Best practices for radiative cooling. *Nature Sustainability* **2023,** *6* (9), 1030-1032. http://dx.doi.org/10.1038/s41893-023-01170-0

100.   Song, Q.; Tran, T.; Herrmann, K.; Lauster, T.; Breitenbach, M.; Retsch, M., A tailored indoor setup for reproducible passive daytime cooling characterization. *Cell Reports Physical Science* **2022,** *3* (8), 100986. https://doi.org/10.1016/j.xcrp.2022.100986

101.   Park, G.; Roh, K.; Kim, H.; Khan, S.; Lee, M.; Kim, B.-W.; Kim, W., Universal Experimental Methods for Evaluating the Performance of Radiative Cooling Materials. *Advanced Materials Technologies* **2022,** *7* (6), 2101205. https://doi.org/10.1002/admt.202101205